2015

Studies on the total synthesis of a new largazole analogue as a potential histone deacetylase inhibitor

Robert Liam Farrell
University of Toledo

A Thesis

entitled

Studies on the Total Synthesis of a New Largazole Analogue as a Potential Histone Deacetylase Inhibitor

by

Robert Farrell

Submitted to the Graduate Faculty as partial fulfillment of the requirements for the

Master of Science Degree in

Medicinal Chemistry

_____

L. M. Viranga Tillekeratne, Ph.D., Committee Chair

_____

Amanda C. Bryant-Friedrich, Ph.D., Committee Member

_____

Zahoor Shah, Ph.D., Committee Member

_____

Patricia R. Komuniecki, PhD, Dean
College of Graduate Studies

The University of Toledo

December 2015

An Abstract of

Studies on the Total Synthesis of a New Largazole Analogue as a Potential Histone Deacetylase Inhibitor

by

Robert Farrell

Submitted to the Graduate Faculty as partial fulfillment of the requirements for the Master of Science Degree in Medicinal Chemistry

The University of Toledo

December 2015

Cancer is a general term used to describe a group of over 100 different diseases all of which have a similar characteristic about them; the out of control abnormal growing of cells. Cancer kills over half a million people every year in the United States and is on the rise. Thus the need for new cancer therapies is also on the rise. It has been shown that histone deacetylases (HDACs) are over expressed in cancer tissues and therefore, inhibiting them is considered to be a way to slow down the progression or stop the spread of cancer in the body. However HDACs are involved in many other cellular functions in the body and indiscriminately inhibiting them would be undesirable. Isoform or class selective HDAC inhibitors targeted to specific HDAC proteins are therefore required.

Natural products are known for being an excellent source of bioactive agents with diverse structure and varying biological activity. They constitute one of the most useful sources of lead molecules for treating a variety of human diseases and disorders. From 1940s to most recent data collected in 2012, of the 175 small molecule drugs approved for treating cancer, 131 or 75% are either natural products or directly derived from them.

To date, there are four HDAC inhibitors approved for treating cancer, but most are non-specific pan-inhibitors. Vorinostat (SAHA) and romidepsin are two HDAC inhibitors that have been approved for the treatment of CTCL. SAHA binds to the Zn^{2+} ion of the HDAC protein without having much interaction with the surface of the protein, while romidepsin has a large surface binding group along with the Zn^{2+} binding moiety, which may account for its higher class I selectivity. Largazole is a potent HDAC inhibitor that has both a Zn^{2+} binding group and a large surface recognition group which may account for its class I selectivity.

Taking largazole as a lead structure, our lab is interested in the synthesis of analogues as potentially more selective HDAC inhibitors by modifying the cyclic group of the molecule. The synthetic approach for one of the analogues **RF1** was successfully developed in the lab. In this molecule the thiazole ring is replaced with a pyridine and the thiazoline ring is replaced with a 4-methylbenzyl amine group. This approach provides a means to synthesize larger quantities of the compound for biological studies.

I would like to dedicate this thesis to my family, my friends, and everyone who has supported me. Without your continued support I do not know if I would have been able to finish my studies.

I love you all very much.

Acknowledgements

I would like to express the deepest appreciation and gratitude to my advisor Dr. Tillekeratne. He has been the one who pushed me through my time in his lab, always making sure I was putting out my best work. Without his guidance and support I don't know if I would have been able to finish in this timely manner if at all. I would also like to thank him for the trust he puts in me in the lab. His passion for chemistry is very contagious and has rubbed off on me. I was extremely fortunate to have you as an advisor and I hope I can go off to make you proud.

I would also like to thank the other people who without their hard work, I would probably not have been able to get everything done. First I would like to start with my committee members Dr. Bryant-Friedrich and Dr. Shah. You both have been there for me for support and guidance even back when I was still an undergraduate. Next I would like to thank our NMR expert, Dr. Kim, for without his continued work to keep the NMR's maintained and running I would not have been able to get the beautiful spectra and would have been very difficult to finish my work. I would like to thank Tony in the stockroom as he was very instrumental in making sure that our lab stayed stocked with the materials we needed and making sure we knew when packages arrived promptly on time. Finally I would like to thank UT and the College of Graduate Studies for accepting me into the program and for giving me this chance to show what I could do.

Table of Contents

List of Figures

List of Schemes

List of Spectra

List of Abbreviations

APL.....Acute promyelocytic leukemia

$CDCl_3$.....Deuterated chloroform
CTCL .....Cutaneous T-cell lymphoma

DCC .....Dicyclohexylcarbodiimide
DCM .....Dichloromethane
DIBAl-H .....Diisobytlaluminium hydride
DIPEA.....Diisopropylethylamine, (Hunig's base)
DMAP.....Dimethylaminopyridine
DMF.....Dimethylformamide
DNA.....Deoxyribonucleic acid

EtOAc .....Ethyl acetate

FDA.....Food and drug administration
Fmoc 9*H*-Fluoren-9-ylmethoxycarbonyl

HATU .....O-(7-Azabenzoriazole-1-yl)-N,N,N'N'-tetramethyluronium hexafluorophosphate
HDAC .....Histone deacetlyase
HOAt.....1-Hydroxy-7-azabenzotriazole

NAD^+ .....Nicotinamide adenine dinucleotide
NCI.....National Cancer Institute
NMR .....Nuclear magnetic resonance

$p21^{WAF1}$ .....Cyclin-dependent kinase inhibitor 1
PTCL.....Peripheral T-cell lymphoma

RAR-PLZF.....Retinoic acid receptor for promyelocytic leukemia zinc finger
RAR-PML.....Retinoic acid receptor for promyelocytic leukemia
RAREs .....Retinoic acid-responsive elements

SAHA.....Suberanilohydroxamic acid
SAR.....Structure activity relationship

TBAF .....Tetra-*n*-butylammonium fluoride
TFA .....Trifluoroacetic acid
THF .....Tetrahydrofuran
TIPS .....Triisopropylsilane
TSA .....Trichostatin A

UT .....The University of Toledo

VPA.....Valproic acid

Chapter 1

Histone Deacetylases Proteins

1.1 Role of HDACs in Cancer

Cancer is a generic name given to a group of over 100 different diseases. Although there are many different types of cancer, they are all characterized by abnormal cells growing out of control. Cancer untreated can lead to serious illness and eventually death. In normal cells, when the DNA of the cell is damaged, the damage is either repaired or the cell dies by apoptosis (Figure 1). In cancer cells when the DNA is damaged, instead of the damage being repaired or the cell undergoing apoptosis, it will continue to grow and divide and eventually invade other tissues. These new cells that are formed will also have the damaged DNA. Sadly, most cancers cannot be prevented because the damage of DNA is caused by a mistake that is made when the normal cell is reproducing. Some external factors that have been proven to trigger uncontrolled cell division and cause cancer are cigarette smoke and sun exposure, but it is almost impossible to tell what caused one person's particular cancer.[7]

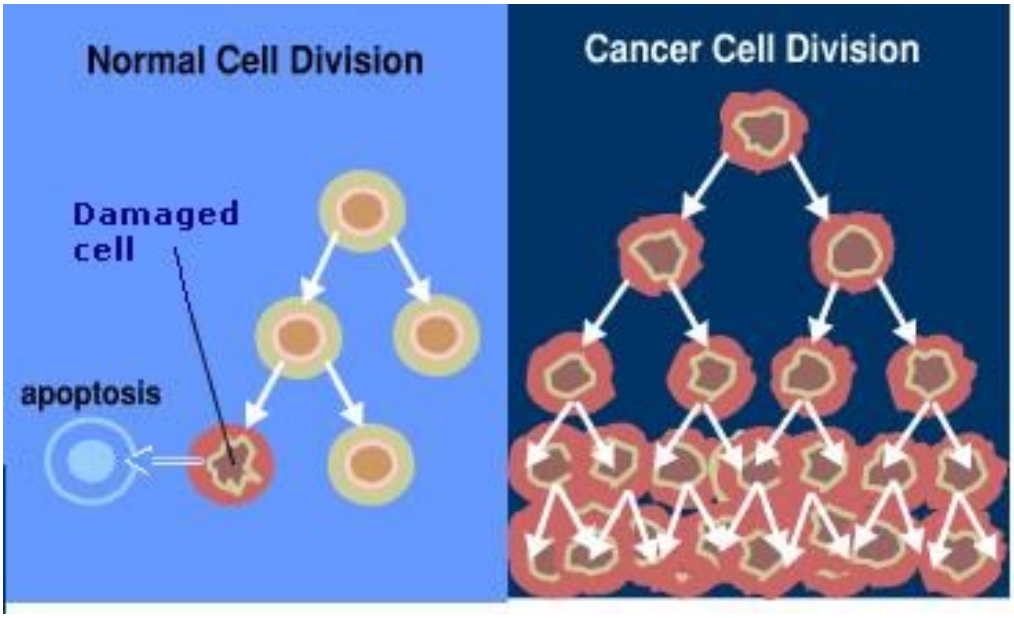

Figure 1. Comparison of normal cell and cancer cell division. Reprinted from http://www.ch.ic.ac.uk/local/projects/burgoine/origins.txt.html

Cancer is the second leading cause of death in the United States.[8] The American Cancer Society estimates that there will be 589,430 deaths caused by cancer in 2015.[9] Therefore, new targets for cancer therapy need to be investigated. It has been shown that certain histone deacetylases (HDAC) are overexpressed in different types of cancers. HDACs are a class of enzymes that remove the acetyl groups from lysine amino acids on histone proteins, allowing the histones to wrap DNA more tightly (Figure 2). The deacetlyated lysine amino groups undergo protonation under physiological conditions and interact with negatively charged DNA phosphate groups to form transcriptionally inactive chromatin. HDAC enzymes in humans comprise of 18 different isoforms that are separated into four classes based on their size, cellular localization, number of catalytic sites, and homology to yeast HDAC proteins.[1a, 10] These four classes are: class I encompassing HDAC1, HDAC2, HDAC3, and HDAC8; class IIA encompassing

HDAC4, HDAC5, HDAC7, and HDAC9; class IIB encompassing HDAC6 and HDAC10; and class IV encompassing HDAC11.[1b, 10] These are classical HDACs that require Zn^{2+} for their enzymatic activity.[11] The other seven are sirtuins which are generally classified as class III HDACs and are NAD^{+} dependent, while also lacking active site Zn^{2+} ion.[11]

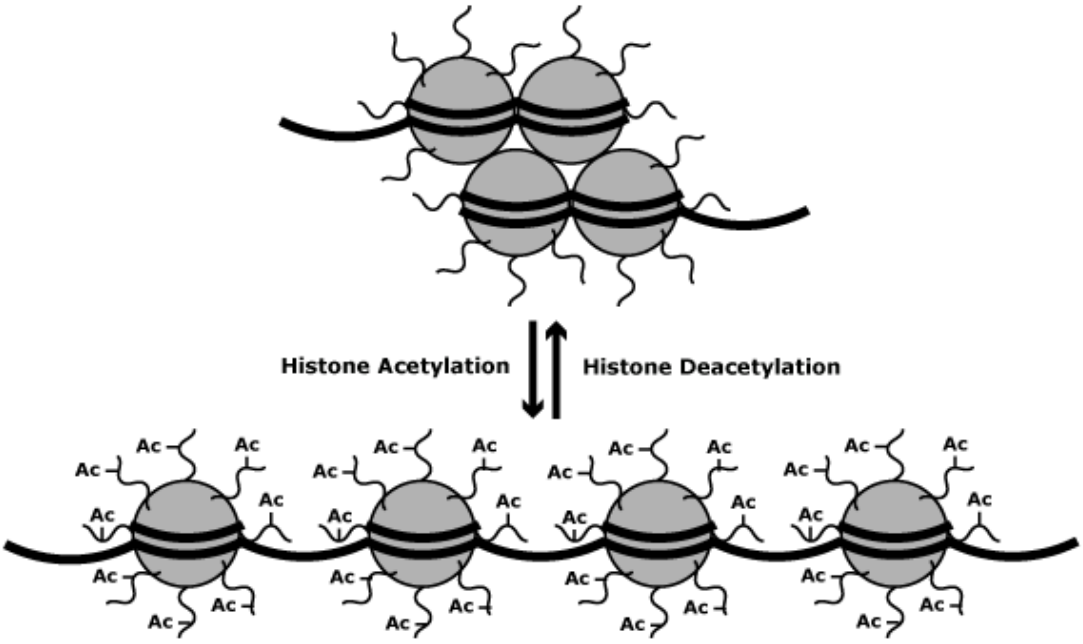

Figure 2. Histone Acetylation and Deacetylation. Reprinted from University of California San Francisco, School of Medicine, Office of Educational Technology, http://missinglink.ucsf.edu/lm/genes_and_genomes/acetylation.html

Class I HDACs, except for HDAC8,[11] are found in large multisubunit complexes that interact with a variety of different transcription factors.[11] It has been evaluated that HDAC1 and HDAC2 must have originated from a common ancestor because they exhibit a high sequence homology of 87% amino acid matching in mice.[11] HDAC3 also shares a

homologous catalytic domain with HDAC1 and HDAC2, but has its major differences in the CK2 phosphorylation site.[11]

Class I HDACs are expressed ubiquitously in mammals, suggesting that they play an important role in enzymatic transcription repression.[11] Universal deletion of these enzymes has led to early embryonic lethality in mice due to severe proliferation defects and retardation during development.

Distinct class I and class II HDAC proteins are overexpressed in certain cancers such as prostate cancer (HDAC1),[11-12] ovarian cancer (HDAC1-3), gastric cancer (HDAC1 and 2), colon cancer (HDAC1, 3, and 6) and lung cancer (HDAC1 and 3).[8, 12] HDAC8 was also identified to be a crucial regulator of tumorigenesis in neuroblastoma cells.[11] However, a molecular mechanism that directly links HDAC activity to cancer formation has yet to be discovered.[10] Small-molecule inhibitors that have the capacity to interfere with HDAC activity have shown significant antitumor effects in pre-clinical cancer trials.[13]

Deregulation of histone acetylation, which is a characteristic of human cancer cells, is a fatal consequence of gene transcription-deregulation. Most of the mechanisms involved in histone hypoacetylation are not well understood. However, available data shows that there is more than one mechanism by which HDACs play a role in cancer development and survival. In acute promyelocytic leukemia (APL), chromosomal translocation produces fusion proteins containing RAR-PML and RAR-PLZF.[12] These fusion proteins activate retinoic acid-responsive elements (RAREs) and recruit the HDAC repressor complex with very high affinity. This prevents the binding of retinoic

acid and thus represses the expression of genes that normally regulate differentiation and proliferation of the myeloid cells. Thus HDACs are a key part of APL development.[12] A common phenomenon in tumor cell onset and progression is transcriptional repression of tumor-suppressor genes by over-expression of HDACs. For example, the cyclin-dependent kinase inhibitor $p21^{WAF1}$ inhibits cell-cycle progression by not allowing the cell to move past the G_0 phase of the cell cycle. In some tumor cells, $p21^{WAF1}$ is inactivated by hypoacetylation of the promoter, and treatment with HDAC inhibitors increases the acetylation of the promoter and gene expression, blocking the tumor cells ability to grow.[12] Another example is the transcription factor Snail which recruits HDAC1, HDAC2, and the corepressor complex mSin3A to the E-cadherin promoter to repress its expression. Down regulation of E-cadherin is thought to increase the invasive potential of carcinomas. Therefore, HDAC inhibitors may be useful to inhibit cancer cell invasion and metastasis.[12]

The role of HDACs in cancer though is not strictly limited to histone deacetylation; they have been found to have a role in deacetylation of non-histone proteins as well. It has been shown that in certain cancer cell types, class I HDACs have a loss of function mutation that may contribute to cancer development. Some tumor-suppressor genes such as Rb require the recruitment of class I HDACs to repress gene transcription. The loss of class I HDAC activity could then induce the expression of the genes that were once repressed by Rb. A mutation of HDAC2 has been discovered in sporadic tumors with microsatellite instability in which loss of HDAC2 expression and activity have led to inability to regulate tumor growth (Figure 3). Though we don't fully

understand the molecular mechanisms underlying the loss of activity of HDAC2s in cancer development, this suggests that it could induce oncogene expression.[12]

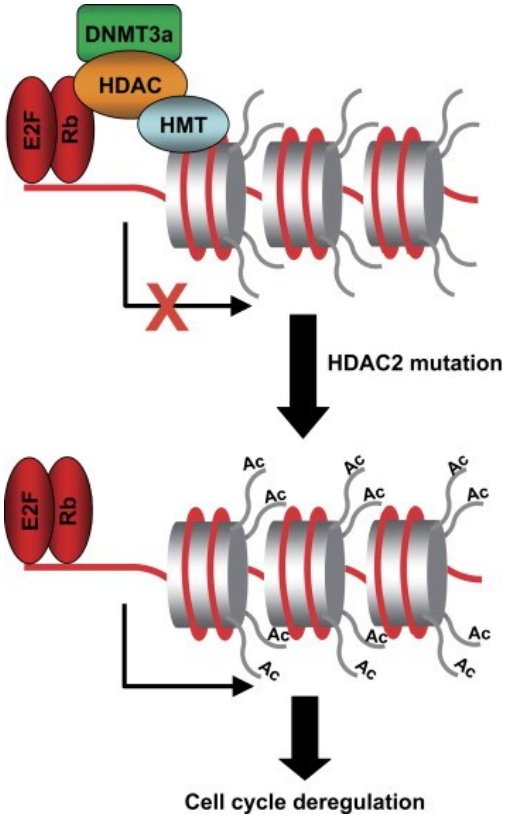

Figure 3. Model showing the possible effect that a HDAC2 mutation could have on cell cycle regulation. Reprinted with permission from *Molecualr Oncology* **2007,** 1 (1), 19-25.

1.2 HDAC Inhibitors

Development of cancer chemotherapy drugs is challenging because of the need for a drug to be selective against cancer cells without affecting normal healthy cells. Natural products have been a main source of lead molecules in the development of anticancer agents;[14] a sample of natural product-based drugs are vincristine, vinblastine, paclitaxel, docetaxel, etoposide, teniposide, topotecan, itinotecan, actinomycin D, and

doxorubicin, most of which have different mechanisms of action. A major issue with big blockbuster drugs such as paclitaxel and actinomycin D (Figure 4) is the development of multiple drug resistance when used for cancer treatment. Therefore, there is a need for newer, more potent, and more selective anticancer drugs.

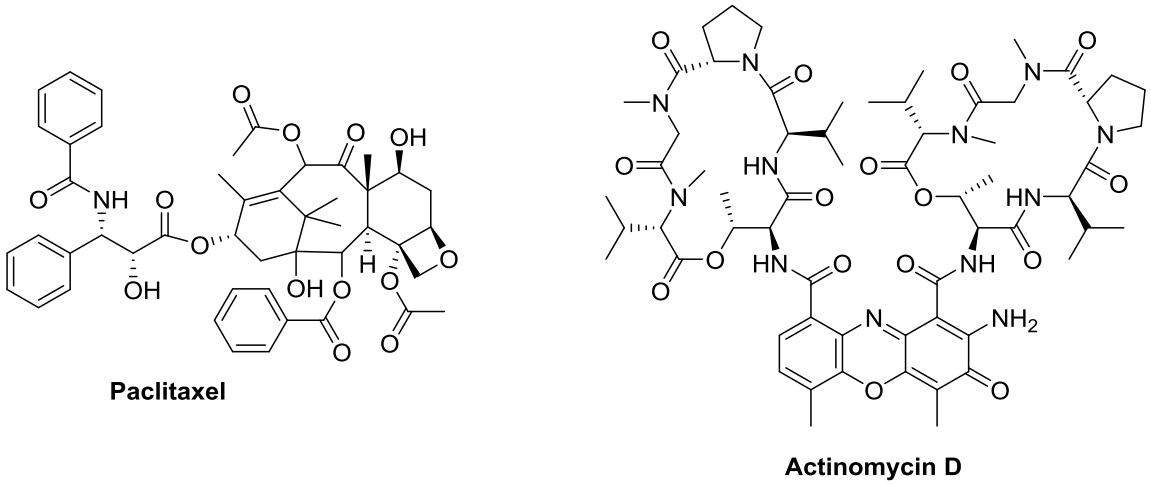

Figure 4. Paclitaxel and Acinomycin D

Small molecule HDAC inhibitors gained traction in the research community after it was discovered that in vitro proliferation of tumor cells is impaired by HDAC inhibitors. It was also found that several HDACs were overexpressed in different tumor cells and cancer cells, suggesting that their suppression could affect the life of a cancer cell.[11] This sparked great interest in HDAC inhibitors for their possible reach into the therapeutic field.

Chemically, HDAC inhibitors can be subdivided into four main structural groups. (I) hydroxamic acids: eg. trichostatin A (TSA)[11], suberanilohydroxamic acid (SAHA), panobinostat, and belinostat; (II) short chain carboxylic acids: eg. phenylbutyrate and valproic acid (VPA); (III) the benzamides: eg. entinostat[11]; and (IV) the cyclic tetrapeptides; eg. romidepsin. All of these HDAC inhibitors target the deacetylase

enzymatic activity of HDAC by binding and competing for the Zn^{2+} **BLANK BLANK** active site. Once bound to the active site, the substrate pocket is blocked and the enzyme becomes deactivated, thus causing an increase in acetylation of histone molecules.[11] In addition to the metal binding functional group, the inhibitors also have a cap group that interacts with amino acids at the entrance to the substrate pocket. It has been found that variations in this cap group can help with selectivity.[10]

To date there are four HDAC inhibitors approved by the US FDA for the treatment of cancer. They are suberanilohydroxamic acid or SAHA (Vorinostat) for the treatment of cutaneous T cell lymphoma (CTCL)[10, 15], romidepsin (Istodax) for the treatment of CTCL[16], panobinostat (Farydak)[17] for the treatment of multiple myeloma[18], and belinostat (Beleodaq)[19] for the treatment of peripheral T-cell lymphoma (PTCL)[20] (Figure 5). Another drug, chidamide (Epidaza), has been approved in China for the treatment of pancreatic cancer and is in clinical trials in the USA. All these approved drugs are pan-HDAC inhibitors, except for romidepsin, which means that they inhibit all classes of HDACs. Romidepsin is a Class I selective HDAC inhibitor.

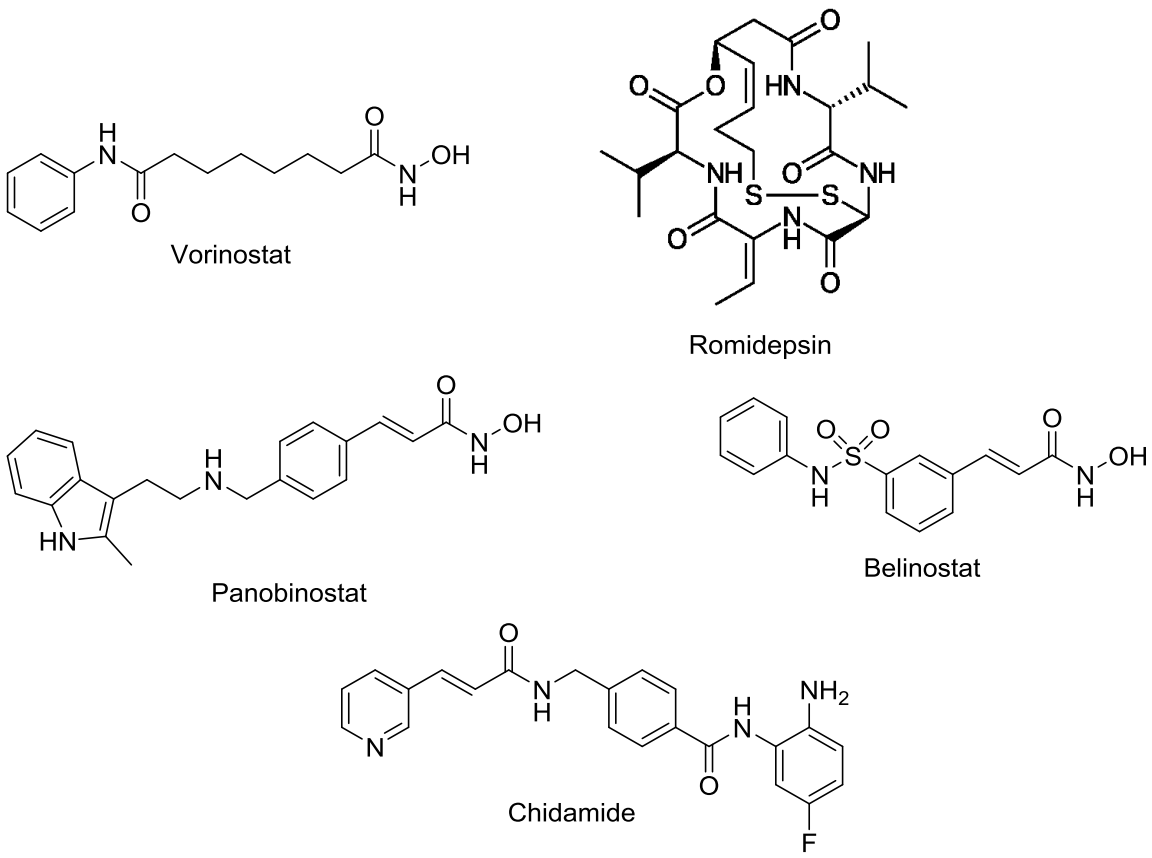

Figure. 5. Clinically used HDAC inhibitors

1.3 Largazole

Largazole (Figure 6) is an HDAC inhibitor isolated by Dr. Luesch's lab from a deep sea marine cyanobacterium of the genus *Symploca* off the coast of Florida.[5b] Largazole derived its name from the place where the bacterium was collected (Key Largo) and from some of its structural features; the two "azole" functional groups. It is a prodrug, with the thioester being hydrolyzed into the active thiol form in vivo.[5b]

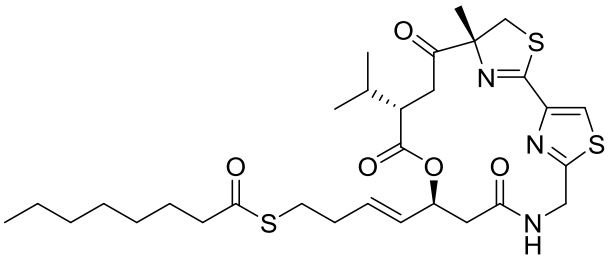

Figure 6. Largazole

Largazole was found to inhibit the growth of numerous epithelial and fibroblastic cancer cells, such as colorectal carcinoma, breast cancer, neuroblastoma and osteosarcoma in nanomolar concentration, while non-transformed cells were inhibited to a much lesser extent. The selectivity was more pronounced than with paclitaxel and some of the other clinically used cancer drugs. In the National Cancer Institute's (NCI) 60-cell line screen, largazole and analogues were found to be cell type specific and have lower general cytotoxic effects. Largazole and analogues have been tested against colorectal carcinoma, human malignant melanoma, human epitheilial carcinoma, breast cancer, lung cancer, prostate cancer, and leukemia cell lines with positive results. These tests confirm that largazole has a broad-spectrum effect, yet is specific against various cancer cell types.[5b]

Largazole as a prodrug was found to be stable in aqueous conditions at a multitude of pH's, but when placed in plasma or cellular proteins, it is quickly hydrolyzed into the thiol.[21] This led to suggest that largazole activation is induced through a general protein assisted mechanism, and even HDAC enzymes themselves are able to catalyze the hydrolysis. This may be the reason for similar levels of activity observed with largazole and largazole thiol in cellular assays.[5b]

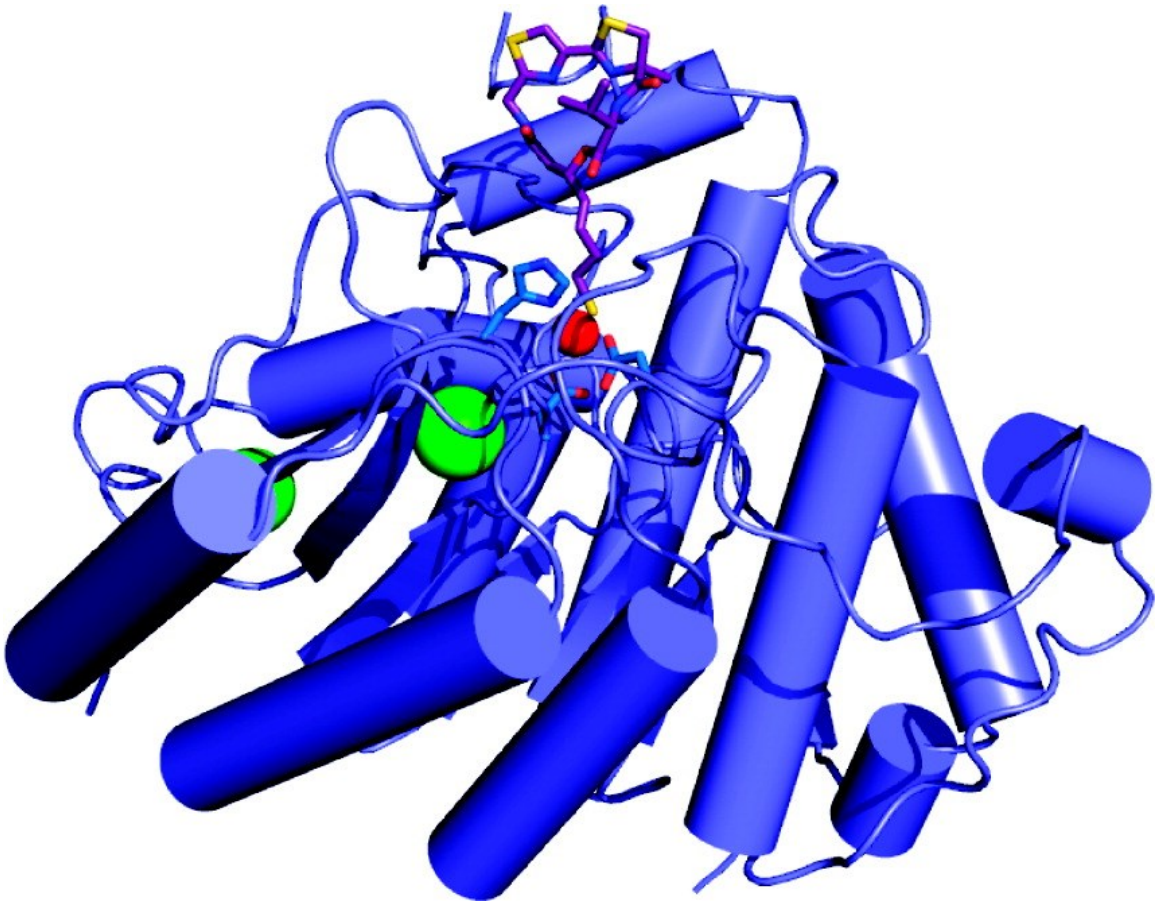

Figure 7. X-ray crystal structure of the HDAC8-largazole thiol complex. "Reprinted with permission *J. Am. Chem. Soc.*, **2011**, *133* (32), pp 12474–12477. Copyright 2011 American Chemical Society."

X-ray crystal structure of HDAC8 complexed with largazole thiol has been reported,[22] (Figure 7) and it is the first crystal structure of an HDAC complexed with a macrocyclic depsipeptide inhibitor. The X-ray crystal structure showed that the 16 membered macrocycle did not undergo any major conformational changes when bound to HDAC8.[22b] In contrast, considerable conformational changes occurred in HDAC8 to accommodate the large inhibitor molecule. The thiol side chain extends in to the Zn^{2+} binding site and formed a tight thiolate-Zn^{2+} interaction. The X-ray crystal structure

revealed that an ideal Zn^{2+} binding geometry is crucial for largazole's exceptionally high binding affinity and biological activity. The crystal structure shows that the macrocyclic portion provides interactions with amino acids on the enzyme surface, which could be exploited to increase isoform selectivity.[5b]

Luesch and Hong described that largazole, while having non-differential selectivity to HDAC1-3, inhibited HDAC8 much less than HDAC11, and among the different class II HDACs (both IIa and IIb) only HDAC10 was severely compromised in vitro.[5b] Numerous structure-activity relationship (SAR) studies on largazole have revealed that different parts of the structure can be optimized to yield better selectivity. Main structural changes have been carried out are in the thioester linker region, the L-valine subunit, and the 4 methylthiazoline-thiazole subunit. Changing the length of the thiol side chain or changing the olefin geometry from *E* to *Z* results in significant loss of activity.[3] Along with changing the C17 configuration from S to R, all these structural changes compromised the binding affinity of the molecule in the HDAC8-largazole thiol complex.[2] Several other metal binding motifs have been made to replace the thioester, such as α-aminobenzamide, α-thioamide, 2-thiomethyl pyridine, 2-thiomethyl thiophene, and 2-thiomethyl phenol groups, but all these changes caused significant decrease in potency compared to largazole.[1b, 5b, 23]

In contrast, replacing the L-valine subunit of largazole with other amino acids, such as L-tyrosine, L-alanine, or glycine was well tolerated. In the HDAC8-largazole thiol complex, the L-valine subunit faces the solvent and doesn't directly influence the enzyme-inhibitor interaction. This means that any other L-amino acid should be tolerated at this position as long as it does not change the overall conformation of the macrocyclic

core. Replacing the L-valine with a D-valine has shown promising results in prostate cancer cells[24], but no other cancer cell line tests have been published. It is suggested that replacing L-valine with a D-amino acid would most likely suffer decreased activity due to change of conformation.[5b]

The methyl group of the 4-methylthiazoline moiety is not necessary for binding of largazole and it can be replaced with a hydrogen atom, an ethyl, or a benzyl group without any significant effect on biological activity. In the HDAC8-largazole thiol complex this methyl group sits parallel to the protein surface and has not direct interaction with the protein, and this may account for the absence of significant effect on biological activity accompanying change at this position. Simplifying the 4-methylthiazoline moiety with a simpler α-aminoisobutyric acid helped to reduce some of the steric strain on the macrocyclic core. This resulted in nano-molar HDAC inhibition, showing that further simplification of the largazole scaffold could be possible without loss of activity as long as the overall conformation was maintained. Willaims group reported the synthesis of a largazole analogue in which the thiazole ring was replaced with a pyridine ring, which lead to enhanced potency.[5b] Our laboratory replaced both the thiazole and the 4-methylthiazoline groups with pyridine rings and the resulting analogue yielded increased potency and class I selectivity (unpublished data) (Figure 8). In this analogue, the sp^3 hybridized carbon at the C-7 position is replaced with a sp^2 carbon atom of the pyridine ring. This modification did not compromise the activity of the molecule.

Our laboratory also synthesizes the analogue **JA3** in which the thiazole was replaced with a pyridine ring and the methylthiazoline was replaced with a methyl amine group (Figure 9). In this analogue, sp^3 hybridization at C7 is retained, but the sp^2

hybridized nitrogen atom of thiazoline ring is replaced with a sp^3 nitrogen of a methyl amine group. These structural modifications resulted in a significant loss of activity. However, replacing the methylamine group with a benzylamine group helped to regain some of the lost activity. Interestingly, although analogue **JA3** was less potent then largazole in the cell growth inhibition assay, it was also less selective with increased inhibitory activity on HDAC6 (unpublished data). We therefore hypothesized that it may be possible to modulate selectivity by structural alteration at this position. Therefore, we decided to synthesize a series of analogues with substituted benzylamine groups to study the effect of changing the electronic properties of the group on activity, including selectivity.

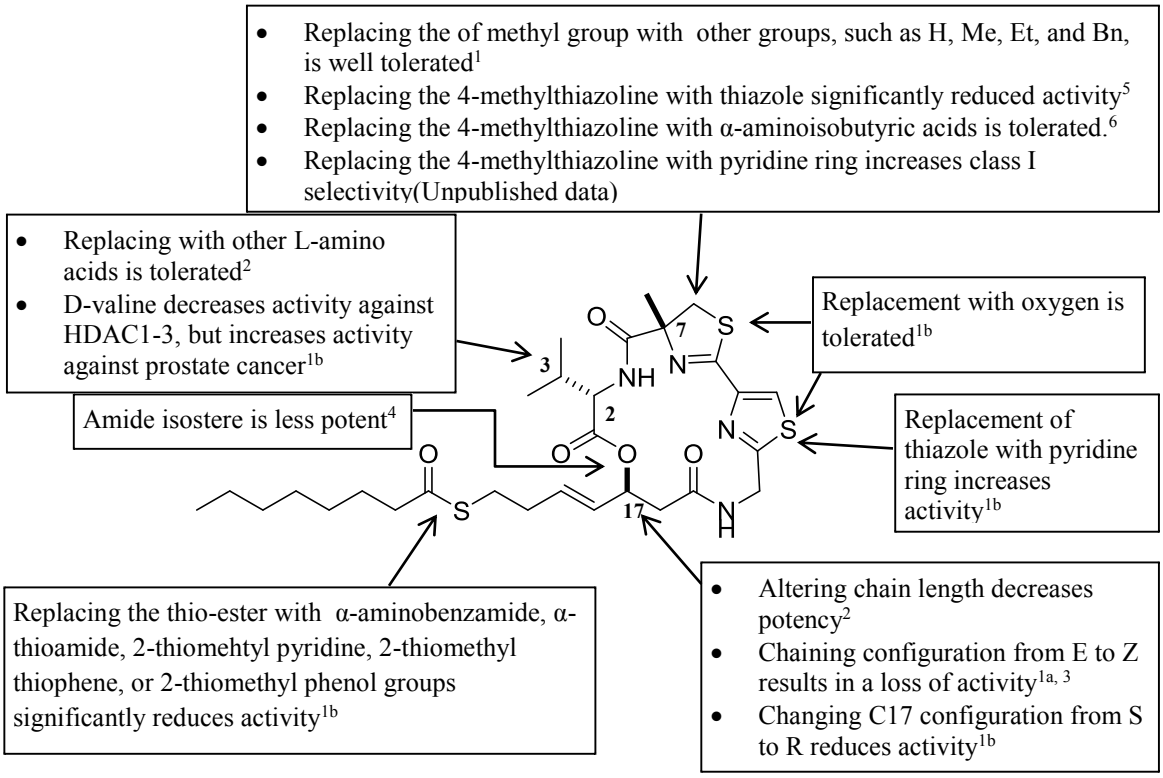

Figure 8. SAR of largazole

In this context, the synthesis of one of the analogue, **S-((E)-4-((7S,10S)-7-isopropyl-3-(4-methylbenzyl)-5,8,12-trioxo-9-oxa-3,6,13-triaza-1(2,6)-pyridinacyclotetradecaphane-10-yl)but-3-en-1-yl) octanethioate (RF1)** is discussed in this thesis**.** In **RF1**, we have maintained the basic scaffold of largazole the same; the thioester sidechain, the *E* configuration of the olefinic side chain along with the S conformation at C17 carbon, and amino acid L-valine. We also retained the sp^2 carbon at C7. The thiazole group has been replaced with a pyridine ring which has already been reported to give an increase in activity.[1b] The methylamine group of **JA3** is replaced with a 4-methylbenzyl amine group to alter hydrophobic properties of this moiety.

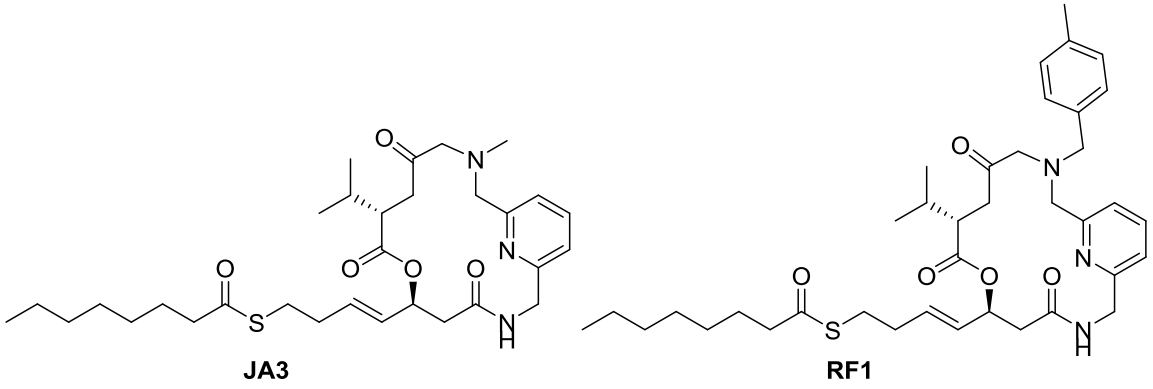

Figure 9. JA3 and RF1

Chapter 2

Results and Discussion

2.1 Retrosynthetic analysis of largazole analogue RF1

The retrosynthetic approach shown in Scheme 1 was utilized for the synthesis of **RF1**. It can be made from the intermediate **23** after removal of protecting groups and cyclization. Intermediate **23** is formed by Yamagushi esterification with Fmoc-valine of the product obtained by acyl transfer from alcohol **13** to amine **20**. Alcohol **13** is formed by aldol reaction of acetyl Nagao **3** with aldehyde **8**.

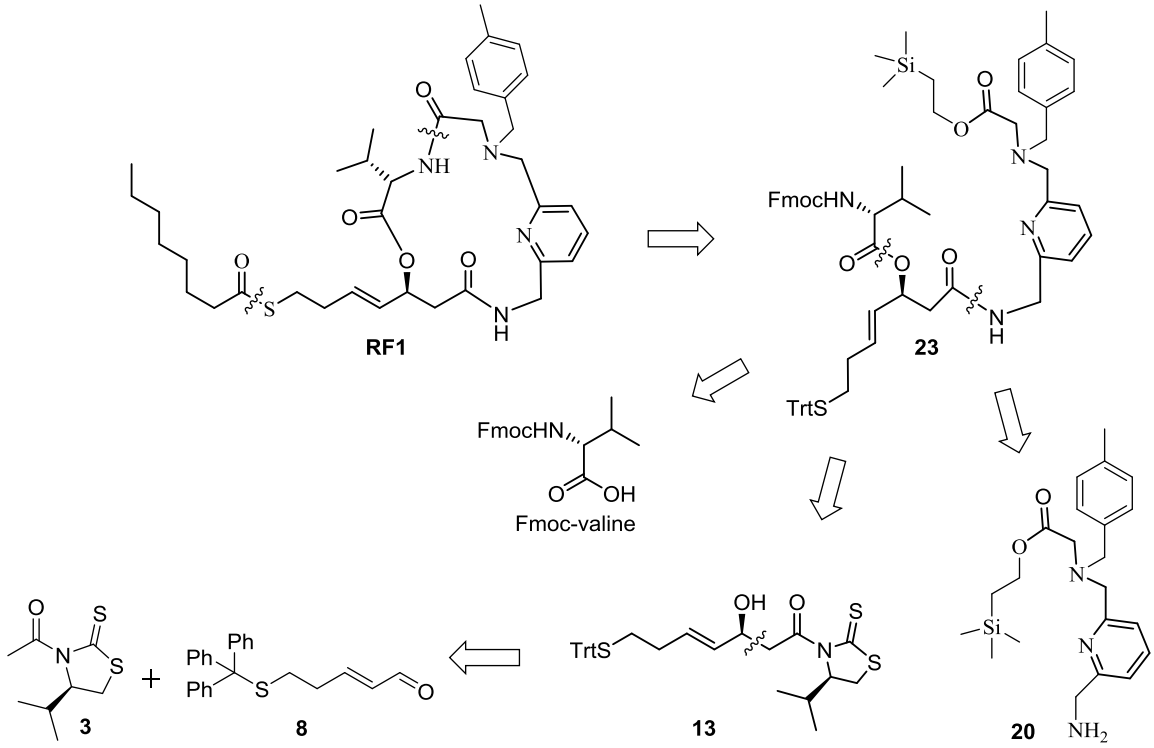

Scheme 1. Retrosynthetic analysis of largazole analogue RF1

2.2 Synthesis of acetyl Nagao auxiliary 3

Acetyl Nagao auxiliary **3** for the stereoselective aldol reaction was made from D-valinol in two steps with an overall yield of 67 % (Scheme 2). In the first step, D-valinol **1** was reacted with carbon disulfide in the presence of KOH under reflux conditions and the crude was purified by chromatography on silica gel to yield Nagao auxiliary **2** in 93 % yield. Nagao auxiliary **2** was reacted with NaH and acetyl chloride at 0°C to give the acetyl Nagao auxiliary **3** in 72 % yield after purification by silica gel chromatography.

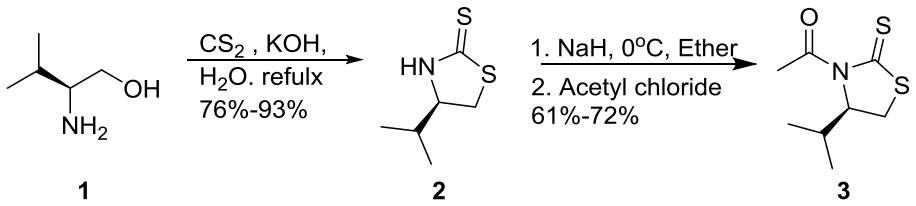

Scheme 2. Synthesis of acetyl Nagao auxiliary **3.**

2.3 Synthesis of alcohol 13

Aldehyde **8** required for the synthesis of alcohol **13** was made using a method that was optimized in our lab (Scheme 3). Michael addition of triphenylmethylmercaptan **4** to acrolein **5** gave aldehyde **6** in 85 % yield. It was used in the next step without further purification. Aldehyde **6** was then subjected to a Wittig reaction with commercially available (cyanomethylene)-triphenylphosphorane to yield an E/Z mixture of the nitrile **7** in 72 % yields. Reduction of the nitrile **7** with DIBAl-H gave an E/Z mixture of aldehyde **8**, which after passing slowly through a silica column in 100 % DCM under gravity was transformed completely to the *E*-aldehyde **8,** which was obtained 70 % yield. The overall yield over three steps was 42 %.

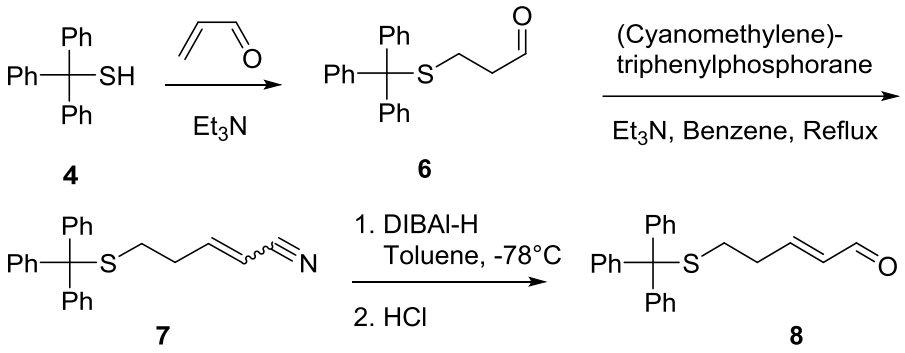

Scheme 3. Synthesis of aldehyde **8**.

Alcohol **13** was synthesized by diastereoselective aldol reaction of the acetyl Nagao auxiliary **3** with aldehyde **8** at -78°C (Scheme 4), followed by flash chromatography purification of the crude product on silica gel to yield the (*S*)-alcohol **13** in 69 % yield.

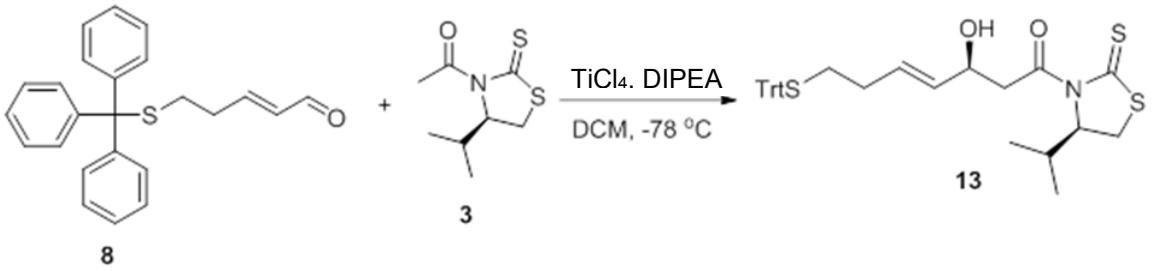

Scheme 4. Synthesis of alcohol **13**.

2.4 Synthesis of amine 20

The synthesis of amine moiety **20** is shown in schemes 5, 6, and 7. Reaction of 2,6-pyridinedimethanol **9** with tosyl chloride in the presence of silver oxide and potassium iodide suspended in dichloromethane yielded mostly the mono-tosylated product **10** with a little di-tosylated product (Scheme 5). They were easily separated by flash chromatography on silica gel in 10 % ethyl acetate in dichloromethane. This reaction yielded 55 % of the monotosyl pyridine **10**. Nucleophilic displacement of the tosyl group of **10** with sodium azide in DMF, after work up, gave the azide **11** in 94 % yield. Azide **11** was converted to the tosyl derivative **12** by a second tosylation reaction with tosyl chloride. Purification of the crude product on a silica plug in ethyl acetate-DCM yielded compound **12** in quantitative yield.

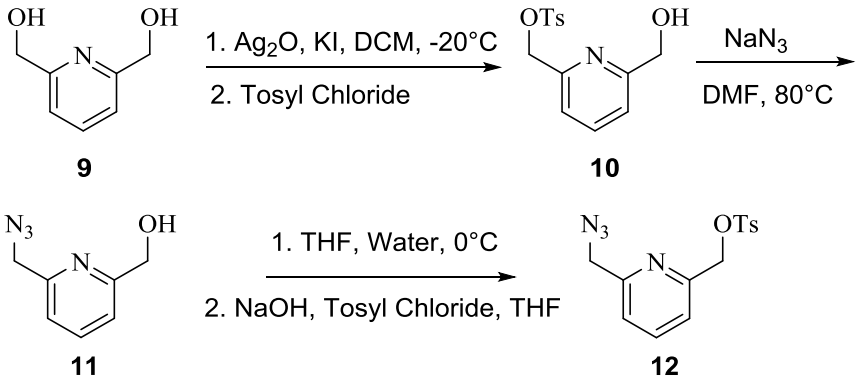

Scheme 5. Synthesis of pyridine tosyl azide **12**.

The secondary amine intermediate **18** was synthesized (Scheme 6) starting with esterification of commercially available 2-bromoacetic acid **14** with 2-(trimethylsilyl)ethanol **15** using DCC as the coupling agent. Purification of the crude product on a silica plug gave 2-(trimethylsilyl)ethyl 2-bromoacetate **16** in 95 % yield. It was reacted with commercially available 4-methylbenzylamine **17** to obtain, after purification by passing through a silica plug in 20 % ethyl acetate in hexanes, the secondary amine **18** in moderate yield of 68.4 %.

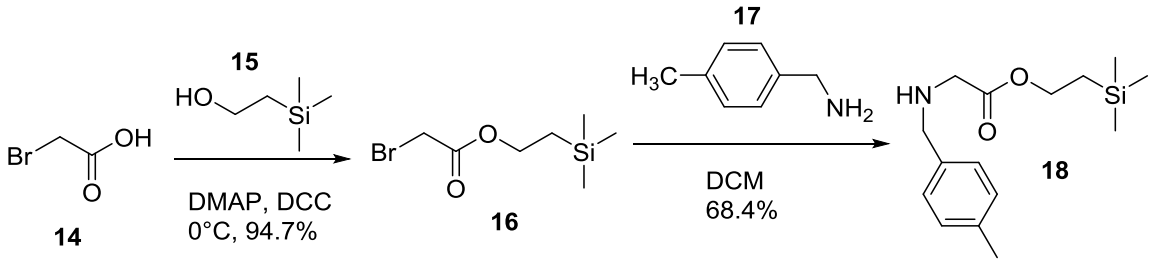

Scheme 6. Synthesis of silyl ester amine **18**.

A simple S_N2 substitution of the tosyl group of **12** by the secondary amine **18** at reflux gave the tertiary amine **19**. After purification by passing through a silica plug in

10 % ethyl acetate in hexanes, the tertiary amine **19** was collected in high yield of 98 %. Finally the azide group **19** was reduced by hydrogenation over Pd catalyst to obtain **20** in 99% yield. The overall yield of amine **20** synthesis was 18.4 %

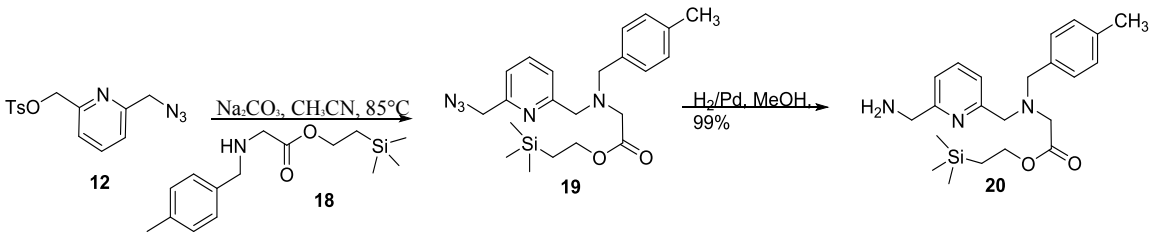

Scheme 7. Synthesis of amine moiety **20**.

2.5 Synthesis of Analogue RF1

With the major fragments required for the synthesis in hand, we proceeded with synthesis of **RF1** as shown in scheme 8. Acyl group transfer from **13** to amine **20** in the presence of DMAP and Hunig's base yielded the amide **21**, which after silica gel chromatography was obtained in 91 % yield. It was subjected to the Yamagushi esterification with Fmoc-valine. After purification by chromatography on silica gel, the product **23** was obtained in 75 % yield. The trimethyl silyl and the Fmoc protecting groups of **23** were removed simultaneously using TBAF. The crude product was washed with hexanes to remove 9- fluorene byproduct. Macrolactamization with HATU, HOAt, and DIPEA in DCM over 2 days, followed by purification of the crude product by column chromatography on silica gel gave only a 12-15% yield of the cyclized molecule **24**. Removal of the trityl group with TFA followed by thioesterification of the resulting thiol with octanoyl chloride with DIPEA in DCM afforded a crude product of **RF1**. The ^{1}H NMR spectrum of the crude showed formation of the final product **RF1**. However, by

final purification by column chromatography on silica gel, it was not possible to seperate sufficient quantities of the final product in pure form for biological testing. However, the approach developed provides a useful method that can be utilized to make larger quantities of the compound for biological studies.

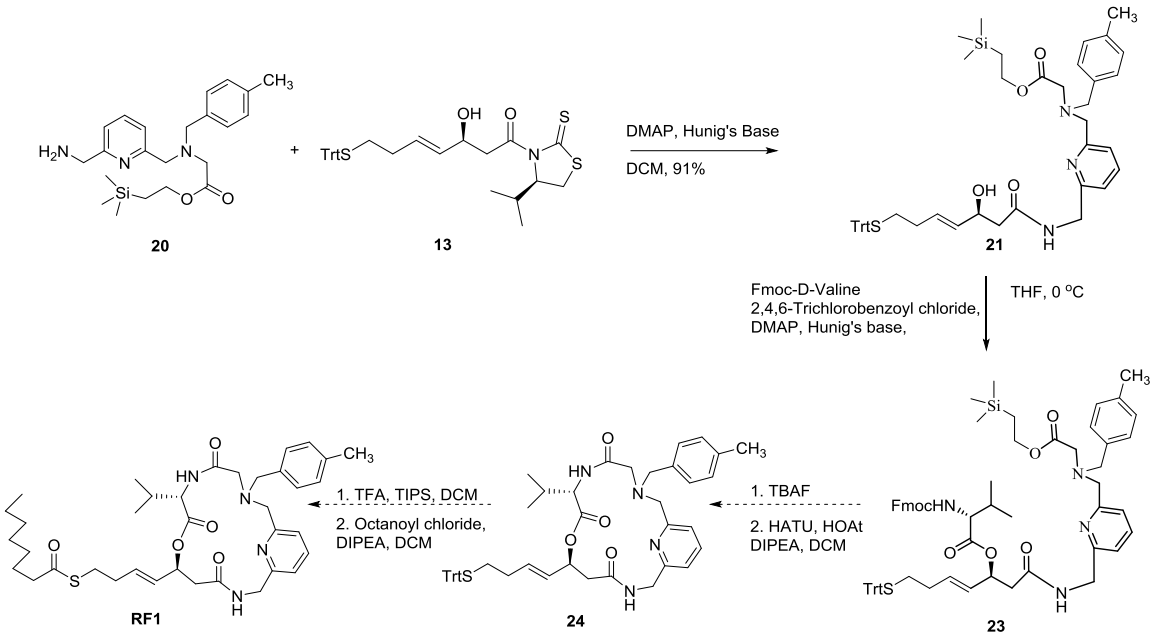

Scheme 8. Synthesis of **RF1**.

2.6 Molecular Modeling of Analogue RF1

General Information

The crystal structures of HDAC1, HDAC2, HDAC4, and HDAC8 were obtained from protein data bank (www.rcsb.org) with pdb id of HDLP1: 1c3s, HDAC2: 4lx2, HDAC4: 4cby and HDAC8: 3rqd. The proteins were prepared by removing all solvent molecules, adding hydrogen atoms, generating Zn^{2+} ionization state and minimizing

energy with OPLS_2005 force field. Only one chain of x-ray structure was retained for docking whenever the structure was polymeric. Glide v 6.1 (Schrodinger, Inc.) was used to generate grids for HDAC proteins without any protein constraints. Maestro v 9.8 (Schrodinger, Inc.) was used to build the ligands and minimize them to obtain the lowest energy conformations, which were docked into the prepared proteins using Glide in extra precision (XP) mode with up to ten poses saved per docked ligand. OPLS_2005 force field was used to calculate the binding free energy and all the docked poses were prepared by PyMol (Schrodinger, New York, NY) (Figure **X**).

Experimental Docking

A docking study of the binding modes of free thiol of **RF1** in the X-ray crystal structure of HDAC1, HDAC2, HDAC4, and HDAC8 enzymes was performed using Glide. The molecular docking analysis revealed that **RF1** free thiol docked into HDAC1 had a binding distance of 4.8 Å between thiol group and zinc ion, which is a poor binding distance compared to largazole thiol's binding distance of 2.3 Å.[22b] When docked into HDAC2 and HDAC8, **RF1** thiol's binding distances between the thiol group and the zinc ion were 2.6 Å and 3.0 Å, respectively. They are both very good binding distances. When **RF1** was docked into HDAC4, no zinc chelation was observed (Figure 10).

The olefinic linker of **RF1** thiol, when inserted into the 11 Å hydrophobic channel of HDAC1, did not form π-π stacking with the phenylalanine residues in the channel as is observed with largazole thiol.[25] However, with HDAC2 and HDAC8, π-π stacking was observed between the olefin and phenylalanine residues. There was no π-π stacking between the olefin and HDAC4.

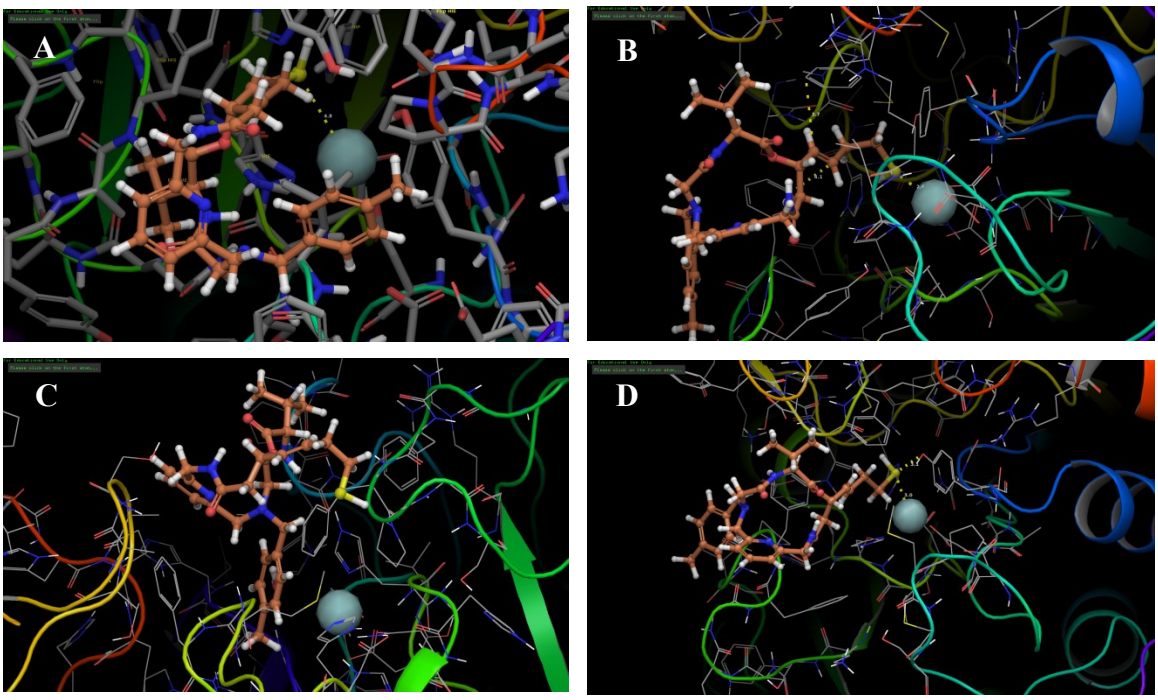

Figure 10: Zinc chelation study of **RF1** bound to HDAC1 (A), HDAC2 (B), HDAC4 (C), and HDAC8 (D)

When looking at the cap binding group of **RF1** bound to HDACs, (Figure 11), significant differences can be seen in the surface binding interactions. With HDAC1, the cap binding group of **RF1** does not seem to be spreading out over the surface to take full advantage of hydrophobic interactions. With HDAC2 and HDAC 8, the 4-methylbenzyl group lies parallel to the surface, possibly taking advantage of either π-π stacking or other hydrophobic interactions. Looking at HDAC4, the thiol is on the surface meaning that the surface residues potentially interact with the thiol group.

The glide score for HDAC1 and **RF1** was -5.081 kcal/mol. The glide score for HDAC2 and **RF1** was -5.312 kcal/mol. The glide score for HDAC4 and **RF1** was -5.012 kcal/mol. The glide score for HDAC8 and **RF1** was -5.445 kcal/mol.

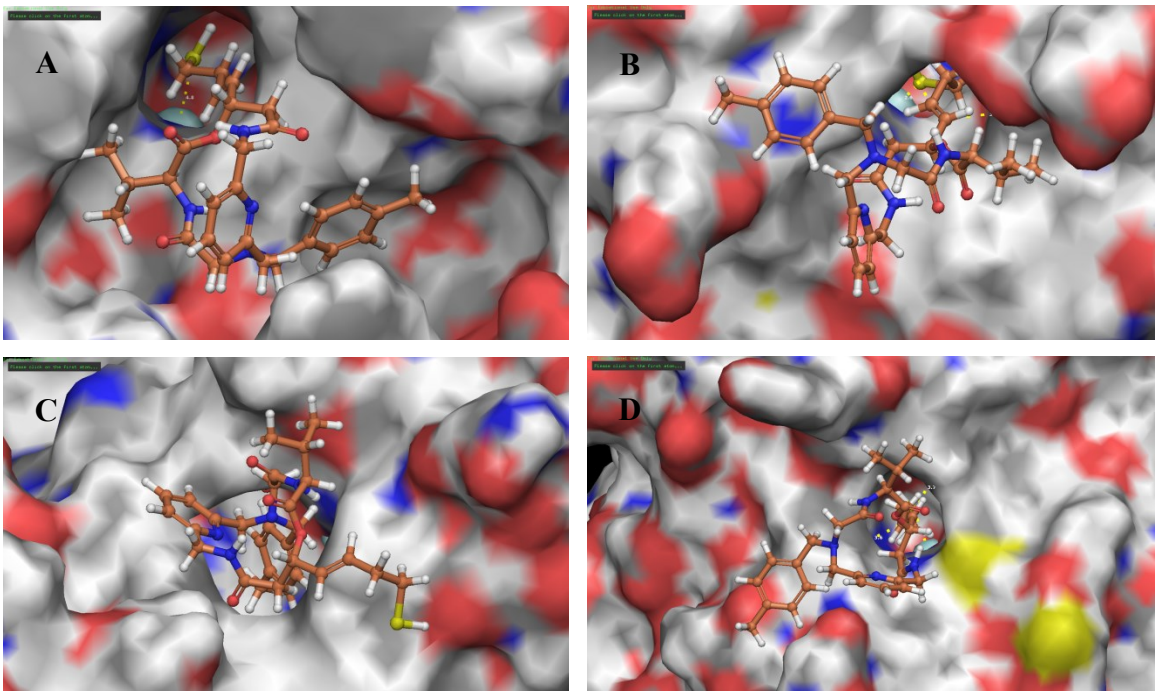

Figure 11: Surface interactions between **RF1** and HDAC1 (A), HDAC2 (B), HDAC4 (C), and HDAC8 (D).

Based on these molecular modeling studies, it seems that **RF1** has the potential for being selective for Class I HDAC2 and HDAC8, but not selective for Class I HDAC1 and Class IIa HDAC4. Thus, **RF1** could be an interesting molecule that is not only likely to be a class I selective HDAC inhibitor, but also could discriminate among HDACs within the same class.

Chapter 3

Experimental Section

General Information

THF and ether were freshly distilled from Na and benzophenone prior to use. NMR spectra were recorded on Varian VXRS 400 MHz, Varian INOVA 600 MHz, and Bruker AVANCE 600 MHz instruments and calibrated using undeuterated solvent as internal reference ($CDCl_3$: ^1H NMR at δ 7.27, ^{13}C NMR at δ 77.36). High-resolution mass spectra (HRMS) were recorded on a Micromass Q-Tof II mass spectrometer at Mass Spectrometry and Proteomics Facility at The Ohio State University, Columbus, Ohio. Crude products were purified by flash column chromatography on silica gel (40-63 μm) purchased from Sorbent Technologies using commercial solvents as specified. Silica gel T.L.C. plates (250 μm) from Dynamic Adsorbents, Inc. were used in thin layer chromatography.

(*R*)-4-Isopropylthiazolidine-2-thione (2). A solution of D-Valinol **1** (4.0 g, 38.77 mmol, 1 eq) was added to 1N aqueous potassium hydroxide solution (200 mL, 200 mmol, 5.15 eq) in a 500 mL round bottom flask. Carbon disulfide, (15.17 g, 199 mmol, 5.14 eq) was added and the reaction mixture was refluxed at 100 ˚C overnight. The solution was cooled to room temperature and extracted with DCM. The combined organic extract was

dried over anhydrous sodium sulfate and concentrated on the rotary evaporator. The residue was passed through a pad of SiO_2 in 75 % DCM/hexanes to yield compound **2** as a white solid, (4.7418 g, 76 %). **^{1}H NMR** (600 MHz, $CDCl_3$): δ 1.00-1.01 (d, *J* = 6.81 Hz, 3H), 1.04-1.05 (d, *J* = 6.74 Hz, 3H), 1.93-2.00 (m, 1H), 3.32-3.35 (dd, *J* = 8.53 Hz, 11.13 Hz, 1H), 3.50-3.53 (dd, *J* = 8.10 Hz, 11.12 Hz, 1H), 4.03-4.05 (m, 1H), 7.44 (s, 1H). **^{13}C NMR** (150 MHz, $CDCl_3$): δ 18.72, 19.23, 32.49, 36.64, 70.22, 201.76 ppm.

(*R*)-1-(4-Isopropyl-2-thioxothiazolidin-3-yl)ethan-1-one (3). To a solution of Nagao auxiliary **2** (2.0 g, 12.4 mmol, 1 eq) in dry ether (50.0 mL) cooled to 0 °C under nitrogen was added NaH, (1.12 g, 28.0 mmol, 2.25 eq) and the mixture was stirred for 1 hour. Acetyl chloride, (1.073 g, 1 mL, 13.7 mmol, 1.1 eq), was added dropwise and the reaction mixture was allowed to warm to room temperature and stirred for 1 hr. 1M HCl (2.5 mL) was added and the mixture was partitioned between EtOAc and water. The organic layer was washed with brine, dried over anhydrous sodium sulfate, and concentrated on the rotary evaporator. The residue was passed through a pad of silica in 50 % DCM in hexanes to yield compound **3** as a yellow oil (1.795g, 71.2 %). **^{1}H NMR** (600 MHz, $CDCl_3$): δ 0.97-0.98 (d, *J* = 6.95 Hz, 3H), 1.05-1.06 (d, *J* = 6.82 Hz, 3H), 2.35-2.38 (dd, *J* = 6.84 Hz, 13.25 Hz, 1H), 2.77 (s, 3H), 3.01-3.03 (dd, *J* = 1.14 Hz, 11.47 Hz, 1H), 3.49-3.52 (dd, *J* = 8.02 Hz, 11.47 Hz, 1H), 5.14-5.16 (m, 1H). **^{13}C NMR** (150 MHz, $CDCl_3$): δ 18.08, 19.40, 27.29, 30.72, 31.10, 71.59, 171.07, 203.57 ppm.

3-(Tritylthio)propanal (6). To a solution of triphenylmethylmercaptan **4** (100 mg, 0.362 mmol, 1 eq) in anhydrous DCM (2 mL) was added acrolein **5** (28.4 mg, 33.84 μL, 0.51

mmol, 1.4 eq) and triethylamine (51.3 mg, 70.6 µL, 0.51 mmol, 1.4 eq). The reaction mixture was stirred at room temperature for 2 h and concentrated under reduced pressure to obtain an off white solid (102.5 mg, 85 %) which was used in the next step without further purification. **^{1}H NMR** (600 MHz, $CDCl_3$): δ 2.35-2.38 (m, 2H), 2.45-2.47 (dt, *J* = 0.75 Hz, 7.14 Hz, 2H), 7.21-7.23 (m, 3H), 7.28-7.30 (t, *J* = 7.69 Hz, 5H), 7.41-7.43 (dd, *J* = 1.22 Hz, 8.49 Hz, 7H), 9.56-9.56 (t, *J* = 1.27 Hz, 1H) **^{13}C NMR** (150 MHz, $CDCl_3$) δ 8.96, 24.72, 43.02, 46.09, 67.32, 127.11, 128.32, 129.88, 144.84, 200.72 ppm.

(*E/Z*)-5-(Tritylthio)pent-2-enenitrile (7). To a solution of (cyanomethylene)-triphenylphosphorane (135.9 mg, 0.451 mmol, 1.5 eq) in anhydrous DCM (2 mL) was added triethylamine (42.6 mg, 58.7 µL, 0.421 mmol, 1.4 eq) over 15 minutes. The reaction mixture was stirred for 45 minutes and concentrated under reduced pressure. Aldehyde 6 (100.0 mg, 0.30 mmol, 1 eq) was added to the residue, followed by anhydrous benzene (2 mL). The reaction mixture was refluxed for 3 h and then concentrated under reduced pressure. The residue was passed through a silica plug in 50 % DCM/hexanes to yield product 7 as an off-white solid (76.3 mg, 71.5 %). **^{1}H NMR** (600 MHz, $CDCl_3$): δ 2.15-2.17 (m, 2H), 2.27-2.31 (m, 2H), 5.17-5.20 (d, *J* = 16.21 Hz, 0.75H), 5.29-5.30 (d, *J* = 7.14 Hz, 0.25H), 6.29-6.33 (dt, *J* = 7.39 Hz, 10.88 Hz, 0.25H), 6.44-6.49 (dt, *J* = 6.91 Hz, 16.27 Hz, 0.75H), 7.23-7.24 (d, *J* = 6.53 Hz, 3H), 7.28-7.31 (m, 6H), 7.40-7.41 (d, *J* = 7.41 Hz, 6H). **^{13}C NMR** (150 MHz, $CDCl_3$): δ 30.07, 32.70, 67.39, 101.37, 117.48, 127.17, 128.33, 129.84, 144.79, 153.64 ppm.

(*E*)-5-(Tritylthio)pent-2-enal (8). A solution of compound **7** (1.0 g, 2.81 mmol, 1 eq) in

toluene (20 mL) was cooled to -78°C under nitrogen. A solution of 1.0 M DIBAl-H (4.22 mg, 3.52 mL, 4.22 mmol, 1.5 eq) was added dropwise and the mixture was stirred for 3 h at -78°C. The reaction mixture was allowed to warm to room temperature, 0.1 M HCl (5 mL) was added dropwise and the mixture was stirred for 15 minutes. It was treated with water and extracted with ethyl acetate. The organic extract was washed with brine, dried over anhydrous sodium sulfate and concentrated on a rotary evaporator. The residue was passed through a silica gel column in 100 % DCM under gravity pressure to yield an off white solid (702.7 mg, 69.7 %). **^{1}H NMR** (600 MHz, $CDCl_3$): δ 2.30-2.32 (t, *J* = 6.78 Hz, 2H), 2.34-2.37 (dd, *J* = 3.78 Hz, 10.80 Hz, 2H), 5.96-6.00 (m, 1H), 6.61-6.66 (dt, *J* = 6.49 Hz, 15.56 Hz, 1H) 7.21-7.24 (m, 3H), 7.28-7.31 (t, *J* = 7.69 Hz, 6H), 7.42-7.73 (dd, *J* = 1.15 Hz, 8.42 Hz, 6H), 9.43-9.44 (d, *J* = 7.86 Hz, 1H). **^{13}C NMR** (150 MHz, $CDCl_3$): δ 30.35, 32.06, 67.33, 127.13, 127.62, 128.06, 128.12, 128.26, 128.28, 128.32, 129.87, 130.02, 133.97, 144.89, 145.58, 156.15, 194.14 ppm.

(*S,E*)-3-Hydroxy-1-((*R*)-4-isopropyl-2-thioxothiazolidin-3-yl)-7-(tritylthio)hept-4-en-1-one (13). To a stirred solution of acetyl Nagao **3** (50 mg, 0.246 mmol, 1 eq) in DCM (2 mL) at 0°C, was added $TiCl_4$ (57.4 mg, 33.3 µL, 0.303 mmol, 1.23 eq). After 5 minutes of stirring, the reaction mixture was cooled to -78°C and DIPEA (39.7 mg, 53.6 µL, 0.3075 mmol, 1.25 eq) was added. The reaction mixture was stirred for 2 h at -78°C and the aldehyde **8** (87.0 mg, 0.243 mmol, 0.987 eq) dissolved in DCM (~.5 mL) was added dropwise. The reaction mixture was stirred at -78°C for 1 h, treated with water (0.5 mL) and diluted with DCM (2.0 mL). The layers were separated and the aqueous layer was extracted with DCM. The combined organic extract was washed with brine,

dried over anhydrous sodium sulfate and concentrated on a rotary evaporator to yield a yellowish oil. It was purified by column chromatography on silica gel in DCM to yield a white solid (94.8 mg, 68.6 %). **^{1}H NMR** (600 MHz, $CDCl_3$): δ 0.96-0.97 (d, *J* = 6.92 Hz, 3H), 1.05-1.06 (d, *J* = 6.80 Hz, 3H), 2.07-2.10 (dd, *J* = 7.16 Hz, 14.31 Hz, 2H), 2.19-2.22 (t, J = 7.34 Hz, 2H), 2.33-2.37 (dd, *J* = 6.75 Hz, 13.44 Hz, 1H), 2.77-2.77 (d, *J* = 4.27 Hz, 1H), 2.99-3.01 (d, *J* = 11.51 Hz, 1H), 3.25-3.29 (dd, *J* = 8.80 Hz, 17.66 Hz, 1H), 3.46-3.49 (dd, *J* = 7.95 Hz, 11.49 Hz, 1H), 3.54-3.58 (dd, *J* = 2.91 Hz, 17.66 Hz, 1H), 4.56-4.56 (d, *J* = 2.94 Hz, 1H), 5.11-5.14 (t, *J* = 6.82 Hz, 1H), 5.44-5.47 (dd, *J* = 6.08 Hz, 15.44 Hz, 1H), 5.56-5.61 (m, 1H), 7.19-7.22 (t, *J* = 7.30 Hz, 3H), 7.27-7.29 (t, *J* = 7.72 Hz, 6H), 7.40-7.41 (d, *J* = 7.41 Hz, 6H). **^{13}C NMR** (150 MHz, $CDCl_3$): δ 18.15, 19.43, 30.05, 30.98, 31.16, 31.71, 31.77, 45.58, 66.89, 68.82, 71.70, 71.73, 126.94, 128.21, 129.93, 130.40, 132.19, 145.21, 172.87, 203.30 ppm.

(6-(Hydroxymethyl)pyridine-2-yl)methyl 4-methylbenzenesulfonate (10). 2,6-Pyridinedimethanol **9** (1.398 g, 10.05 mmol, 1 eq), silver (I) oxide (4.028 g, 17.38 mmol, 1.7 eq), and potassium iodide (0.374 g, 2.93 mmol, 0.3 eq), were suspended in DCM (72 mL) and the mixture was stirred in an ice bath at -20 °C. Tosyl chloride (1.922 g, 10.08 mmol, 1 eq) was added. The reaction mixture was stirred for 30 minutes at the same temperature and then brought to room temperature and stirred for 3 h. The mixture was filtered through a celite pad, washed with EtOAc, and the combined organic solution was concentrated on the rotary evaporator. The residue was subjected to flash column chromatography on SiO_2 in 10 % EtOAc in DCM to yield compound **10** as an orange oil (1.621 g, 55 %). **^{1}H NMR** (600 MHz, $CDCl_3$) δ 2.46 (s, 3H), 4.70 (s, 2H), 5.15 (s, 2H),

7.17-7.19 (d, J = 7.79 Hz, 1H), 7.32-7.33 (d, J = 7.70 Hz, 1H), 7.34-7.35 (d, J = 5.58 Hz, 2H), 7.68-7.71 (t, J = 7.74 Hz, 1H), 7.82-7.84 (d, J = 8.31 Hz, 2H). **^{13}C NMR** (150 MHz, $CDCl_3$): δ 21.7, 63.8, 71.4, 120.2, 120.6, 128.1, 129.9, 132.8, 137.7, 145.1, 152.6, 158.9 ppm.

(6-(Azidomyhyl)pyridine-2-yl)methanol (11). A mixture of compound **10** (1.0 g, 3.417 mmol) and NaN_3 (0.667 g, 10.25 mmol) in DMF (25 mL) was heated at 80 °C for 3 h. The reaction mixture was concentrated on a rotary evaporator. The residue was dissolved in EtOAc and filtered through a celite pad to yield compound **11** as a cloudy orange oil (528.6 mg, 94.2 %). **^{1}H NMR** (600 MHz, $CDCl_3$) δ 4.47 (s, 2H), 4.77 (s, 2H), 7.20-7.26 (dd, J = 7.70 Hz, 21.24 Hz, 2H), 7.71-7.73 (t, J = 7.70 Hz, 1H), 8.08 (s, 1H). **^{13}C NMR**(150 MHz, $CDCl_3$): δ 55.61, 64.20, 120.01, 120.84, 138.04, 155.19, 159.37 ppm.

(6-(Azidomethyl)pyridine-2-yl)methyl 4-methylbenzenesulfonate (12). A solution of compound **11** (1.0 g, 6.05 mmol, 1 eq), in THF (5.5 mL) and water (5.5 mL) was cooled to 0 °C. NaOH (0.71 g, 18.17 mmol, 3 eq), was added to the solution and tosyl chloride (1.27 g, 6.65 mmol, 1.1 eq) in THF (5.5 mL) was added dropwise. The reaction mixture was stirred at 0 °C for 4 h and extracted with DCM. The combined organic extract was washed with brine, dried over anhydrous sodium sulfate, and the solvent was removed on the rotary evaporator. The residue was passed through a silica plug in 20 % EtOAc in DCM to yield compound **12** as a dark orange brown oil (1.379 g, 71.6 %). **^{1}H NMR** (600 MHz, $CDCl_3$) δ 2.46 (s, 3H), 4.41 (s, 2H), 5.14 (s, 2H), 7.20-7.28 (d, J = 6.96 Hz, 1H), 7.35-7.36 (d, J = 8.16 Hz, 2H), 7.39-7.40 (d, J = 7.80 Hz, 1H), 7.73-7.75 (t, J = 7.78 Hz,

1H), 7.84-7.85 (d, *J* = 8.31 Hz, 2H). **^{13}C NMR** (150 MHz, $CDCl_3$): δ 21.7, 55.3, 71.5, 121.0, 121.5, 128.1, 129.9, 132.8, 138.0, 145.0, 153.9, 155.5 ppm.

2-(Trimethylsilyly)ethyl 2-bormoacetate (16). A mixture of 2-bromoacetic acid **14** (5.7 g, 41 mmol, 2.05 eq), DMAP (195.4 mg, 1.6 mmol, 0.08 eq) and DCC (8.66 g, 42 mmol, 2.1 eq) in DCM (40 mL) was cooled to 0°C under nitrogen. 2-(Trimethylsilyl)ethanol **15** (2.36 g, 2.86 mL, 20.0 mmol, 1 eq) was added dropwise. The reaction mixture was stirred at 0°C for 1 h and then was brought to room temperature and stirred overnight. It was filtered and the filter cake was washed with 75 % hexanes/ether followed by a $NaHCO_3$ solution. The organic extract was dried over anhydrous sodium sulfate and concentrated under reduced pressure to give an oil. It was purified by passing through a silica plug in 25 % dichloromethane/hexanes to give 2-(trimethylsilyl)ethyl 2-bromoacetate **16** (3.902 g, 81.6 %) as a clear oil. **^{1}H NMR** (600 MHz, $CDCl_3$) δ 0.02 (s, 9H), 0.98-1.01 (m, *J* = 1.00 Hz, 2H), 3.78 (s, 2H), 4.21-4.24 (m, 2H). **^{13}C NMR** (150 MHz, $CDCl_3$): δ -1.17, 17.56, 26.46, 27.08, 65.16, 167.70 ppm.

2-(Trimethylsilyl)ethyl (4-methylbenzyl)glycinate (18). To a solution of 4-methylbenzylamine **17** (2.42 g, 20.0 mmol, 2 eq, 2.54 mL) in DCM (50 mL) under nitrogen was added 2-(trimethylsilyl)ethyl 2-bromoacetate **16** (2.39 g, 10.0 mmol, 1 eq) dropwise over 5 minutes. The reaction mixture was stirred at room temperature for 2 h and was concentrated under reduced pressure. It was purified by passing through a silica plug in 20 % ethyl acetate/hexanes to give a yellow oil of 2-(trimethylsilyl)ethyl (4-methylbenzyl)glycinate **18** (1.64 g, 6.19 mmol, 62 %). **^{1}H NMR** (600 MHz, $CDCl_3$) δ

0.04 (s, 9H), 0.98-1.01 (m, 2H), 2.33 (s, 3H), 3.40 (s, 2H), 3.82 (s, 2H), 4.20-4.23 (m, 2H), 7.14-7.15 (d, *J* = 7.75 Hz, 2H), 7.24-7.25 (d, *J* = 7.65 Hz, 2H). **^{13}C NMR** (150 MHz, $CDCl_3$): δ -1.17, 17.70, 21.44, 50.50, 53.35, 63.37, 128.59, 129.46, 136.78, 137.09, 172.95 ppm. **HRMS:** (ESI) calculated for $C_{15}H_{26}NO_2Si$ $[M + H]^+$ 280.1733; found 280.1750.

2-(Trimethylsilyl)ethyl N-((6-(azidomethyl)pyridine-2-yl)-N-(4-methylbenzyl)glycinate) (19). A mixture of 2-(trimethylsilyl)ethyl (4-methylbenzyl)glycinate **18** (1.3 g, 4.65 mmol, 1 eq), (6-(azidomethyl)pyridine-2-yl)methyl 4-methylbenzenesulfonate **12** (1.48 g, 4.65 mmol, 1 eq), Na_2CO_3 (1.18 g, 11.16 mmol, 2.4 eq) and acetonitrile (25 mL) was refluxed at 85°C under nitrogen for 3 h. The reaction mixture was cooled to room temperature. It was treated with water and extracted with ethyl acetate. The combined organic extract was dried over anhydrous sodium sulfate and concentrated under reduced pressure. The residue was purified by passing through a silica plug in 10 % ethyl acetate/hexanes to yield the tertiary amine **19**, (2.0 g, 97.8 %). **^{1}H NMR** (400 MHz, $CDCl_3$) δ 0.03 (s, 9H), 0.96-1.01 (m, 2H), 2.32 (s, 3H), 3.33 (s, 2H), 3.78 (s, 2H), 3.93 (s, 2H), 4.16-4.20 (m, 2H), 4.44 (s, 2H), 7.11-7.13 (d, *J* = 7.79, 2H), 7.19-7.21 (d, *J* = 7.54 Hz, 1H), 7.26-7.28 (d, *J* = 7.86, 2H), 7.57-7.59 (d, *J* = 7.70 Hz, 1H), 7.68-7.72 (t, *J* = 7.69 Hz, 1H). **^{13}C NMR** (150 MHz, $CDCl_3$): δ -1.17, 17.77, 21.46, 54.78, 55.93, 58.16, 59.87, 62.99, 120.52, 122.48, 129.30, 129.35, 135.77, 137.15, 137.83, 155.12, 160.36, 171.84 ppm. **HRMS:** (ESI) calculated for $C_{22}H_{32}N_5O_2Si$ $[M + H]^+$ 426.2325; found 426.2335.

2-(Trimethylsilyl)ethyl N-((6-(aminomethyl)pyridine-2-yl)methyl)-N-(4-methylbenzyl)glycinate (20). A mixture of 2-(trimethylsilyl)ethyl N-((6-(azidomethyl)pyridine-2-yl)-N-(4-methylbenzyl)glycinate) **19** (310 mg, 0.728 mmol), 5 % palladium on carbon (38 mg, 0.357 mmol), and methanol (10 mL) was shaken under hydrogen for 5 h. The reaction mixture was passed through a celite pad and concentrated under reduced pressure to yield 2-(trimethylsilyl)ethyl N-((6-(aminomethyl)pyridine-2-yl)methyl)-N-(4-methylbenzyl)glycinate **20** (288 mg, 99 %). **^{1}H NMR** (600 MHz, $CDCl_3$) δ 0.28 (s, 9H), 0.97-0.10 (m, 2H), 2.32 (s, 3H), 3.33 (s, 2H), 3.49 (s, 2H), 3.78 (s, 2H), 3.92 (s, 2H), 3.95 (s, 2H), 4.18-4.20 (m, 2H), 7.11-7.12 (d, *J* = 7.76 Hz, 3H), 7.26-7.28 (d, *J* = 7.95 Hz, 2H), 7.46-7.47 (d, *J* = 7.69 Hz, 1H), 7.61-7.64 (t, *J* = 7.65 Hz, 1H). **^{13}C NMR** (150 MHz, $CDCl_3$) δ 1.17, 17.77, 21.46, 47.90, 54.75, 58.14, 59.99, 62.96, 119.78, 121.34, 129.30, 135.86, 137.11, 137.43, 159.59, 160.94, 171.92 ppm.

2-(Trimethylsilyl)ethyl (*S,E*)-N-((6-((3-hydroxy-7-(tritylthio)hept-4-enamido)methyl)pyridine-2-yl)methyl)-N-(4-methylbenzyl)glycinate (21). A mixture of compound **20**, (320 mg, 0.80 mmol, 1.2 eq), DMAP (82 mg, 0.667 mmol, 1 eq), Hunig's base (86.2 mg, 116 µL, 0.667 mmol, 1 eq) and DCM (6 mL) was stirred under nitrogen for 30 minutes. A solution of compound **13** (375.5 mg, 0.667 mmol, 1 eq) in DCM (6 mL) was added dropwise and the reaction mixture was stirred for 3 h. The reaction mixture was concentrated under reduced pressure and the residue was purified by silica plug with 75 % EtOAc/hexanes to yield product **21** (517.7mg, 91%) as a yellow oil. **^{1}H NMR** (600 MHz, $CDCl_3$) δ 0.03 (s, 9H), 0.96-0.99 (m, 2H), 1.25-1.27 (t, *J* = 7.15 Hz, 1H), 2.05 (s, 2H), 2.18-2.21 (t, *J* = 7.47 Hz, 2H), 2.32 (s, 3H), 2.37-2.41 (dd, *J*

= 9.05 Hz, 15.00 Hz, 1H), 2.45-2.48 (dd, *J* = 2.97 Hz, 13.97 Hz, 1H), 3.32 (s, 2H), 3.77 (s, 2H), 3.91 (s, 2H), 4.11-4.14 (q, *J* = 7.15 Hz, 1H), 4.16-4.19 (m, 2H), 4.44-4.49 (dd, *J* = 6.03 Hz, 22.50 Hz, 2H), 4.56-4.60 (dd, *J* = 5.23 Hz, 16.48 Hz, 1H), 5.41-5.45 (dd, *J* = 6.75, 15.94, 1H), 5.55-5.60 (m, 1H), 7.07-7.09 (d, *J* = 7.87 Hz, 2H), 7.11-7.12 (d, *J* = 7.73 Hz, 2H), 7.18-7.21 (m, 3H), 7.25-7.28 (m, 9H), 7.39-7.39 (d, *J* = 1.07 Hz, 2H), 7.40-7.40 (d, *J* = 1.31 Hz, 2H), 7.46-7.47 (d, *J* = 7.61 Hz, 1H), 7.62-7.65 (t, *J* = 7.68 Hz, 1H). **^{13}C NMR** (150 MHz, $CDCl_3$) δ 1.16, 14.54, 17.78, 21.41, 21.47, 31.74, 31.81, 43.15, 44.41, 54.76, 58.21, 59.65, 60.75, 63.05, 66.88, 69.49, 120.54, 121.94, 126.92, 128.19, 129.24, 129.38, 129.91, 130.07, 132.78, 135.72, 137.20, 137.68, 145.22, 155.36, 159.35, 171.52, 171.97, 172.33 ppm. **HRMS:** (ESI) calculated for $C_{48}H_{58}N_3O_4SSi$ $[M + H]^+$ 800.3917; found 800.3917.

(*S,E*)-1-(((6-(((4-methylbenzyl)(2-oxo-2-(2-(trimethylsilyl)ethoxy)ethyl)amino)methyl)pyridin-2-yl)methyl)amino)-1-oxo-7-(tritylthio)hept-4-en-3-yl (((9H-fluoren-9-yl)methoxy)carbonyl)-D-valinate (23). To a solution of Fmoc-L-valine **22** (54.3 mg, 0.16mmol, 2eq) in THF (1 mL) at 0°C under nitrogen were added, Hunig's base (31.0 mg, 41.8 µL, 0.24 mmol, 3 eq) and 2,4,6-tricholorobenzoyl chloride (41 mg, 64 µL, 0.168 mmol, 2.1 eq) and the mixture was stirred for 1 h. When TLC showed the formation of product, a solution of compound **21** (64 mg, 0.08 mmol, 1 eq) and DMAP (9.8 mg, 0.08 mmol, 1 eq) in THF (1 mL) was added to the reaction mixture at 0°C. It was then allowed to warm to room temperature

and stirred overnight. The reaction mixture was concentrated on a rotary evaporator and the residue was separated by flash chromatography on silica gel in 10-100 % acetone/hexanes to yield a dark orange oil (66.9 mg, 74.6%). **^{1}H NMR** (600 MHz, $CDCl_3$): δ 0.03 (s, 9H), 0.79-0.80 (d, *J* = 6.86 Hz, 3H), 0.88-0.90 (d, *J* = 6.82 Hz, 3H), 0.97-1.00 (m, 2H), 2.03-2.06 (q, *J* = 7.01 Hz, 2H), 2.15-2.18 (m, 2H), 2.32 (s, 3H), 2.54-2.58 (dd, *J* = 5.11 Hz, 14.57 Hz, 1H), 2.62-2.66 (dd, *J* = 7.69 Hz, 14.43 Hz, 1H), 3.34 (s, 2H), 3.80 (s, 2H), 3.94 (s, 2H), 4.17-4.21 (d, *J* = 8.30 Hz, 16.74 Hz, 4H), 4.30-4.36 (m, 2H), 4.48 (s, 2H), 5.35-5.44 (m, 2H), 5.66-5.71 (m, 2H), 7.04-7.05 (d, *J* = 7.05 Hz, 1H), 7.11-7.12 (d, *J* = 7.73 Hz, 2H), 7.18-7.21 (t, *J* = 7.24 Hz, 3H), 7.26-7.28 (t, *J* = 7.49 Hz, 8H), 7.29-7.32 (t, *J* = 7.42 Hz, 2H), 7.38-7.39 (d, *J* = 7.76 Hz, 8H), 7.46-7.47 (d, *J* = 7.66 Hz, 1H), 7.57-7.60 (dd, *J* = 6.59 Hz, 12.29 Hz, 3H), 7.75-7.76 (d, *J* = 7.19 Hz, 2H). **^{13}C NMR** (150 MHz, $CDCl_3$): δ -1.18, 17.75, 17.78, 19.28, 21.45, 31.43, 31.58, 31.70, 41.86, 44.65, 47.46, 54.65, 58.15, 63.02, 65.46, 67.27, 69.26, 72.88, 120.27, 121.71, 125.43, 126.92, 127.39, 128.01, 128.18, 128.23, 129.25, 129.37, 129.88, 134.15, 141.59, 144.10, 144.23, 145.14, 155.52, 156.52, 168.94, 171.23 ppm. **HRMS:** (ESI) calculated for $C_{68}H_{77}N_4O_7SSi$ $[M + H]^+$ 1121.5282; found 1121.5298.

(7*S*,10*S*)-7-Isopropyl-3-(4-methylbenzyl)-10-((*E*)-4-(tritylthio)but-1-en-1-yl)-9-oxa-3,6,13-triaza-1(2,6)-pyridinacycloetetradecaphane05,8,12-trione (24). To a solution of compound **23** (59.1 mg, 0.054 mmol, 1 eq) in THF (17 mL) under nitrogen was added 1M TBAF (106.7 μL, 0.1067 mmol, 2 eq) dropwise at 0°C. The reaction mixture was allowed to warm to room temperature and stirred for 5 h. After NMR analysis showed

the removal of the silyl group, the reaction mixture was concentrated under reduced pressure and partitioned between ethyl acetate and water. The organic layer was dried over anhydrous sodium sulfate and concentrated on rotary evaporator. The crude residue was washed several times with hexanes. The residue was then dried azeotropically with toluene. To a solution of the residue, HOAt (7.61 mg, 0.0561 mmol, 2 eq), and HATU (21.3 mg, 0.0561 mmol, 2 eq) in anhydrous DCM (22 mL) was added Hunig's base (15.9 mg, 0.123 mmol, 4.4 eq, 21.5 μL) under nitrogen. The reaction mixture was stirred for 2 days. It was concentrated under reduced pressure and separated by flash chromatography on silica gel in 0-30 % acetone/hexanes, followed by reverse phase chromatography in water/acetonitrile to yield an orange oil (8.7 mg, 12.2 %). **^{1}H NMR** (600 MHz, $CDCl_3$): δ 0.91-0.92 (d, *J* = 6.88 Hz, 3H), 0.99-1.00 (d, *J* = 6.87 Hz, 3H), 1.05-1.08 (t, *J* = 6.86 Hz, 2H), 1.38 (s, 2H), 1.48 (s, 4H), 1.96-1.99 (m, 2H), 2.13-2.15 (m, 1H), 2.23-2.25 (dt, impurity), 2.38-2.40 (t, *J* = 7.31 Hz, 2H), 2.44 (s, 3H), 2.84-2.87 (dd, *J* = 3.10 Hz, 14.41 Hz, 1H), 2.92-2.96 (dd, *J* = 10.78 Hz, 14.44 Hz, 1H), 3.05-3.08 (d, impurity), 3.22-3.24 (d, *J* = 16.91, 1H), 3.40-3.43 (d, *J* = 16.93 Hz, 1H), 3.49 (s, 1H), 3.65-3.67 (d, *J* = 13.47 Hz, 1H), 3.80-3.82 (t, *J* = 6.57 Hz, 1H), 3.83-3.86 (d, *J* = 13.50 Hz, 1H), 3.95-3.98 (d, *J* = 13.86 Hz, 2H), 4.11-4.13 (d, *J* = 13.84 Hz, 1H), 4.38-4.41 (dd, *J* = 2.00 Hz, 15.97 Hz, 1H), 4.88-4.91 (dd, *J* = 4.26 Hz, 10.25 Hz, 1H), 5.06-5.10 (dd, *J* = 6.89 Hz, 15.99 Hz, 1H), 5.71-5.74 (dd, *J* = 6.08 Hz, 15.52 Hz, 1H), 5.87-5.91 (m, 2H), 7.29-7.30 (d, *J* = 7.81 Hz, 2H), 7.39-7.42 (t, *J* = 7.32 Hz, 3H), 7.48-7.51 (t, *J* = 7.81 Hz, 9H), 7.59-7.58 (d, *J* = 8.15 Hz, 7H), 7.94-7.96 (t, *J* = 7.64 Hz, 1H), 8.91-8.93 (d, *J* = 10.21 Hz, 1H). **^{13}C NMR** (150 MHz, $CDCl_3$): δ 14.46, 17.45, 19.40, 21.80, 23.02, 29.59, 30.03, 31.34, 31.87, 32.95, 42.61, 44.48, 54.09, 56.31, 57.00, 57.16, 58.14, 60.96, 66.99, 73.32, 121.61,

122.58, 126.94, 127.57, 128.04, 128.06, 128.10, 128.21, 128.25, 128.61, 129.58, 129.89, 130.00, 132.80, 133.72, 135.18, 147.20, 155.87, 157.62, 169.56, 169.78, 170.97 ppm.

***S*-((*E*)-4-((7*S*,10*S*)-7-Isopropyl-3-(4-methylbenzyl)-5,8,12-trioxo-9-oxa-3,6,13-triaza-1(2,6)-pyridinacyclotetradecaphane-10-yl)but-3-en-1-yl) octanethioate (RF1).** A solution of compound **24** (12 mg, 0.015 mmol, 1 eq) and triisopropylsilane (5.95 mg, 7.69 µL, 0.038 mmol, 2.5 eq) in DCM (0.5 mL) was cooled to 0°C. TFA (119.9 mg, 1.05 mmol, 70 eq, 80.5 µL) was added and the reaction mixture was allowed to warm to room temperature and stirred for 4 h at this temperature. The reaction mixture was concentrated under reduced pressure and dried azeotropically with toluene. A solution of DMAP (1.0 mg, 0.00819 mmol, 0.22 eq) in DCM (1 mL) at 0°C was added with Hunig's base (9.7 mg, 13.1 µL, 0.075 mmol, 5 eq) and octanoyl chloride (9.8 mg, 10.3 µL, 0.06 mmol, 4 eq). The reaction mixture was stirred overnight at room temperature and was concentrated under reduced pressure. (3.4 mg, 34 %) **^{1}H NMR** (600 MHz, $CDCl_3$): δ 0.66-0.67 (d, *J* = 6.75 Hz, 3H), 0.80-0.81 (d, *J* = 6.72 Hz, 3H), 0.86-0.88 (t, *J* = 5.99 Hz, 4H), 1.25-1.29 (m, 10H), 1.62-1.64 (m, 4H), 2.17 (s, 1H), 2.32 (s, 5H), 2.50-2.53 (t, *J* = 7.55 Hz, 2H), 2.73-2.74 (d, *J* = 6.40 Hz, 2H), 2.87-2.89 (t, *J* = 7.13 Hz, 2H), 3.16-3.19 (d, *J* = 17.09 Hz, 1H), 3.41-3.44 (d, *J* = 17.12 Hz, 1H), 3.49-3.51 (d, *J* = 13.59 Hz, 1H), 3.67-3.69 (d, *J* = 13.62 Hz, 1H), 3.74-3.76 (d, *J* = 14.16 Hz, 1H), 3.90-3.92 (d, *j* = 14.13 Hz, 1H), 4.47-4.50 (dd, *J* = 3.10 Hz, 16.87 Hz, 1H), 4.64-4.68 (dd, *J* = 3.58 Hz, 16.73 Hz, 1H), 4.88-4.91 (dd, *J* = 3.75 Hz, 10.19 Hz, 1H), 5.53 (dd, *J* = 6.47 Hz, 15.37 Hz, 1H), 5.66-5.67 (d, *J* = 6.38 Hz, 1H), 5.78-5.83 (m, 1H), 7.09-7.10 (d, *J* = 7.57 Hz, 2H), 7.15-7.17 (t, *J* = 7.13 Hz, 2H), 7.20-7.21 (d, *J* 7.60 Hz, 2H), 7.65-7.68 (t, *J* = 7.59 Hz,

1H), 8.80-8.82 (d, *J* = 10.11 Hz, 1H) **^{13}C NMR** (150 MHz, $CDCl_3$): δ 1.36, 12.16, 17.78, 18.91, 30.05, 31.27, 42.37, 42.91, 54.05, 115.70, 117.63, 120.67, 126.13, 127.10, 128.28, 148.63, 149.28, 152.51, 161.23, 161.47, 161.71, 161.95, 197.42 ppm.

References

1. (a) Souto, J. A.; Vaz, E.; Lepore, I.; Pöppler, A.-C.; Franci, G.; Álvarez, R.; Altucci, L.; de Lera, Á. R. Synthesis and Biological Characterization of the Histone Deacetylase Inhibitor Largazole and C7- Modified Analogues. *J. Med. Chem.* **2010,** *53* (12), 4654-4667; (b) Bowers, A. A.; West, N.; Newkirk, T. L.; Troutman-Youngman, A. E.; Schreiber, S. L.; Wiest, O.; Bradner, J. E.; Williams, R. M. Synthesis and Histone Deacetylase Inhibitory Activity of Largazole Analogs: Alteration of the Zinc-Binding Domain and Macrocyclic Scaffold. *Org. Lett.* **2009,** *11* (6), 1301-1304.

2. Ying, Y.; Liu, Y.; Byeon, S. R.; Kim, H.; Luesch, H.; Hong, J. Synthesis and Activity of Largazole Analogues with Linker and Macrocycle Modification. *Org. Lett.* **2008,** *10* (18), 4021-4024.

3. Zeng, X.; Yin, B.; Hu, Z.; Liao, C.; Liu, J.; Li, S.; Li, Z.; Nicklaus, M. C.; Zhou, G.; Jiang, S. Total Synthesis and Biological Evaluation of Largazole and Derivatives with Promising Selectivity for Cancers Cells. *Org. Lett.* **2010,** *12* (6), 1368-1371.

4. Bowers, A. A.; Greshock, T. J.; West, N.; Estiu, G.; Schreiber, S. L.; Wiest, O.; Williams, R. M.; Bradner, J. E. Synthesis and Conformation−Activity Relationships of the Peptide Isosteres of FK228 and Largazole. *J. Am. Chem. Soc.* **2009,** *131* (8), 2900-2905.

5. (a) Chen, F.; Gao, A.-H.; Li, J.; Nan, F.-J. Synthesis and Biological Evaluation of C7-Demethyl Largazole Analogues. *ChemMedChem* **2009,** *4* (8), 1217-1217; (b) Hong, J.; Luesch, H. Largazole: From discovery to broad-spectrum therapy. *Natural Product Reports* **2012,** *29* (4), 449-456.

6. Benelkebir, H.; Marie, S.; Hayden, A. L.; Lyle, J.; Loadman, P. M.; Crabb, S. J.; Packham, G.; Ganesan, A. Total synthesis of largazole and analogues: HDAC inhibition, antiproliferative activity and metabolic stability. *Biorg. Med. Chem.* **2011,** *19* (12), 3650-3658.

7. What is Cancer? http://www.cancer.org/cancer/cancerbasics/what-is-cancer (accessed 7/15/2015).

8. Aldana-Masangkay, G. I.; Sakamoto, K. M. The Role of HDAC6 in Cancer. *Journal of Biomedicine and Biotechnology* **2011,** *2011*, 10.

9. Siegel, R. L.; Miller, K. D.; Jemal, A. Cancer statistics, 2015. *CA Cancer J Clin* **2015,** *65* (1), 5-29.

10. Bieliauskas, A. V.; Pflum, M. K. H. Isoform-selective histone deacetylase inhibitors. *Chem. Soc. Rev.* **2008,** *37* (7), 1402-1413.

11. Reichert, N.; Choukrallah, M.-A.; Matthias, P. Multiple roles of class I HDACs in proliferation, differentiation, and development. *Cellular and Molecular Life Sciences* **2012,** *69* (13), 2173-2187.

12. Ropero, S.; Esteller, M. The role of histone deacetylases (HDACs) in human cancer. *Molecular Oncology* **2007,** *1* (1), 19-25.

13. Minucci, S.; Pelicci, P. G. Histone deacetylase inhibitors and the promise of epigenetic (and more) treatments for cancer. *Nat Rev Cancer* **2006,** *6* (1), 38-51.

14. Cragg, G. M.; Grothaus, P. G.; Newman, D. J. Impact of natural products on developing new anti-cancer agents. *Chem. Rev.* **2009,** *109* (7), 3012-43.

15. Mann, B. S.; Johnson, J. R.; Cohen, M. H.; Justice, R.; Pazdur, R. FDA approval summary: vorinostat for treatment of advanced primary cutaneous T-cell lymphoma. *Oncologist* **2007,** *12* (10), 1247-52.

16. Bertino, E. M.; Otterson, G. A. Romidepsin: a novel histone deacetylase inhibitor for cancer. *Expert Opinion on Investigational Drugs* **2011,** *20* (8), 1151-1158.

17. (a) Richardson, P. G.; Laubach, J. P.; Lonial, S.; Moreau, P.; Yoon, S.-S.; Hungria, V. T.; Dimopoulos, M. A.; Beksac, M.; Alsina, M.; San-Miguel, J. F. Panobinostat: a novel pan-deacetylase inhibitor for the treatment of relapsed or relapsed and refractory multiple myeloma. *Expert Review of Anticancer Therapy* **2015,** *15* (7), 737-748; (b) Berdeja, J. G.; Hart, L. L.; Mace, J. R.; Arrowsmith, E. R.; Essell, J. H.; Owera, R. S.; Hainsworth, J. D.; Flinn, I. W. *Phase I/II study of the combination of panobinostat and carfilzomib in patients with relapsed/refractory multiple myeloma*. 2015; Vol. 100, p 670-676.

18. George, P.; Bali, P.; Annavarapu, S.; Scuto, A.; Fiskus, W.; Guo, F.; Sigua, C.; Sondarva, G.; Moscinski, L.; Atadja, P.; Bhalla, K. *Combination of the histone deacetylase inhibitor LBH589 and the hsp90 inhibitor 17-AAG is highly active against human CML-BC cells and AML cells with activating mutation of FLT-3*. 2005; Vol. 105, p 1768-1776.

19. Plumb, J. A.; Finn, P. W.; Williams, R. J.; Bandara, M. J.; Romero, M. R.; Watkins, C. J.; La Thangue, N. B.; Brown, R. Pharmacodynamic Response and Inhibition

of Growth of Human Tumor Xenografts by the Novel Histone Deacetylase Inhibitor PXD101. *Molecular Cancer Therapeutics* **2003,** *2* (8), 721-728.

20. Falkenberg, K. J.; Johnstone, R. W. Histone deacetylases and their inhibitors in cancer, neurological diseases and immune disorders. *Nat Rev Drug Discov* **2014,** *13* (9), 673-691.

21. Liu, Y.; Salvador, L. A.; Byeon, S.; Ying, Y.; Kwan, J. C.; Law, B. K.; Hong, J.; Luesch, H. Anticolon Cancer Activity of Largazole, a Marine-Derived Tunable Histone Deacetylase Inhibitor. *J. Pharmacol. Exp. Ther.* **2010,** *335* (2), 351-361.

22. (a) Decroos, C.; Clausen, D. J.; Haines, B. E.; Wiest, O.; Williams, R. M.; Christianson, D. W. Variable Active Site Loop Conformations Accommodate the Binding of Macrocyclic Largazole Analogues to HDAC8. *Biochemistry* **2015,** *54* (12), 2126-2135; (b) Cole, K. E.; Dowling, D. P.; Boone, M. A.; Phillips, A. J.; Christianson, D. W. Structural Basis of the Antiproliferative Activity of Largazole, a Depsipeptide Inhibitor of the Histone Deacetylases. *J. Am. Chem. Soc.* **2011,** *133* (32), 12474-12477.

23. Bhansali, P.; Hanigan, C. L.; Casero, R. A.; Tillekeratne, L. M. Largazole and analogues with modified metal-binding motifs targeting histone deacetylases: synthesis and biological evaluation. *J. Med. Chem.* **2011,** *54* (21), 7453-63.

24. Wang, B.; Huang, P.-H.; Chen, C.-S.; Forsyth, C. J. Total Syntheses of the Histone Deacetylase Inhibitors Largazole and 2-epi-Largazole: Application of N-Heterocyclic Carbene Mediated Acylations in Complex Molecule Synthesis. *The Journal of Organic Chemistry* **2011,** *76* (4), 1140-1150.

25. Zhou, J.; Xie, H.; Liu, Z.; Luo, H.-B.; Wu, R. Structure–Function Analysis of the Conserved Tyrosine and Diverse π-Stacking among Class I Histone Deacetylases: A QM

(DFT)/MM MD Study. *Journal of Chemical Information and Modeling* **2014,** *54* (11), 3162-3171.

Appendix A

NMR spectra

(R)-4-isopropylthiazolidine-2-thione (2).

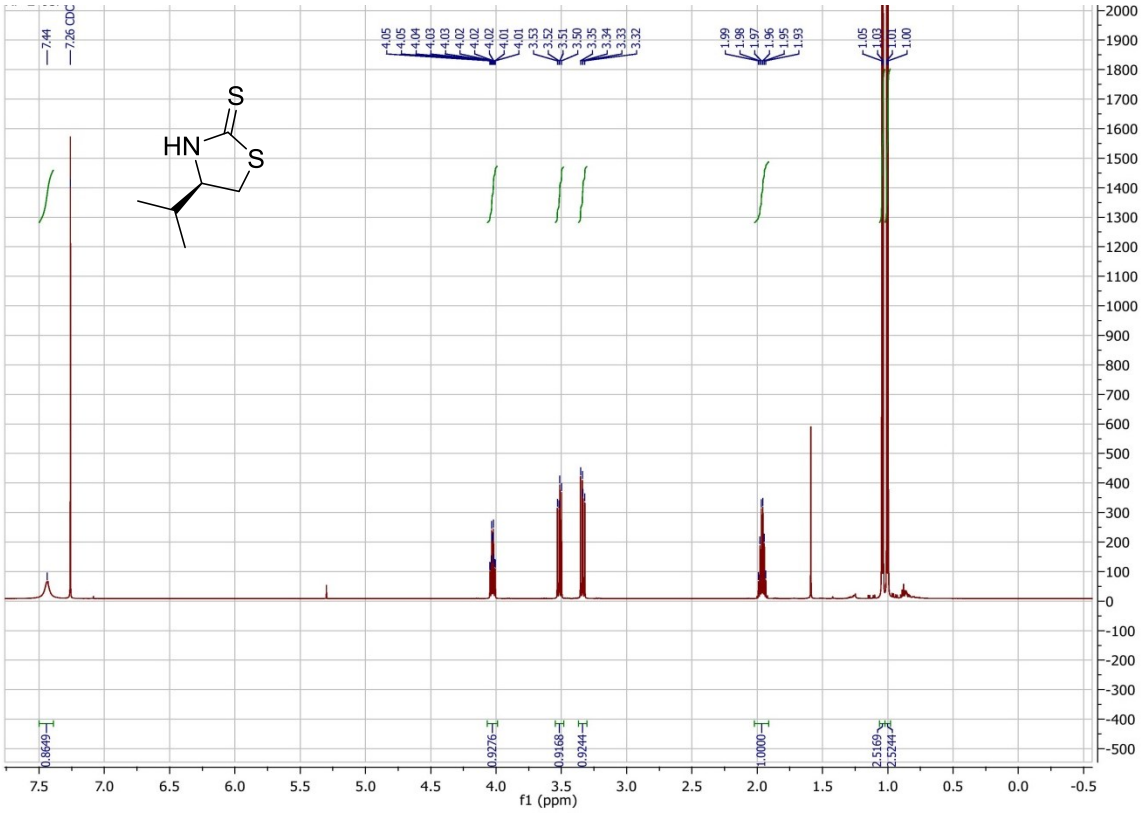

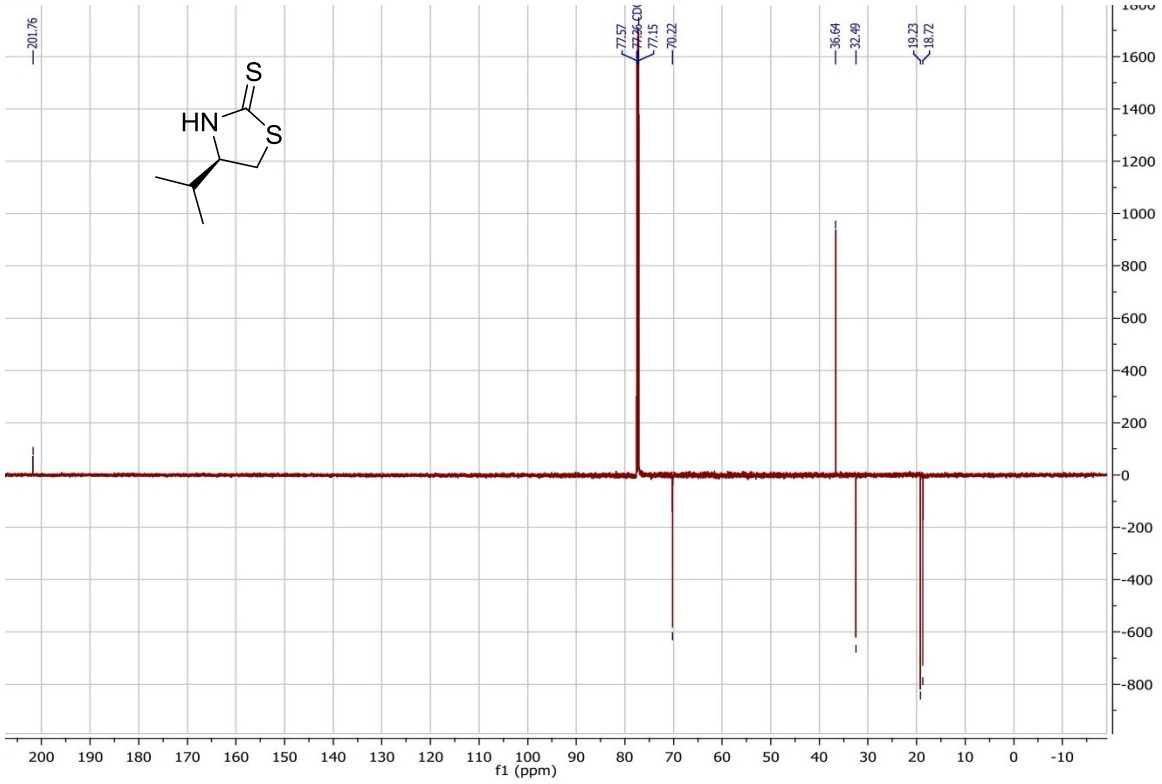
201.76
77.57
77.36-CDCl3
77.15
70.22
36.64
32.49
19.23
18.72
S
HN
S
f1 (ppm)

(R)-1-4-isopropyl-2-thioxothiazolidin-3-yl)ethan-1-one (3).

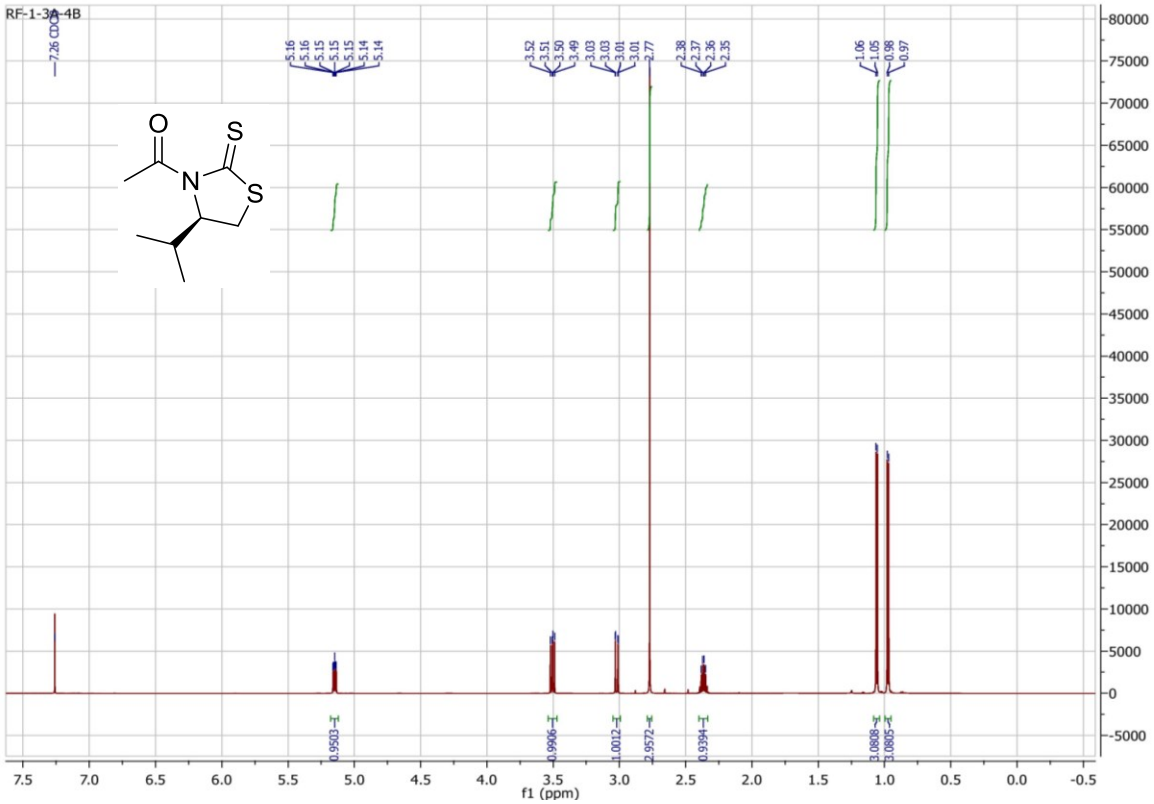

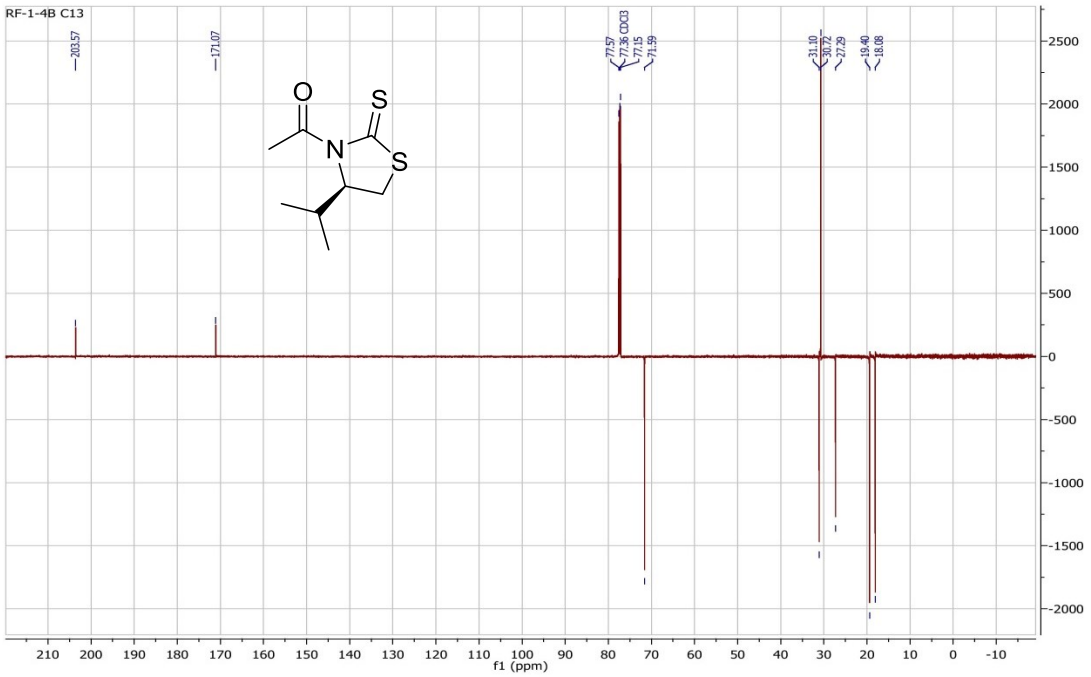

(Tritylthio)propanal (6).

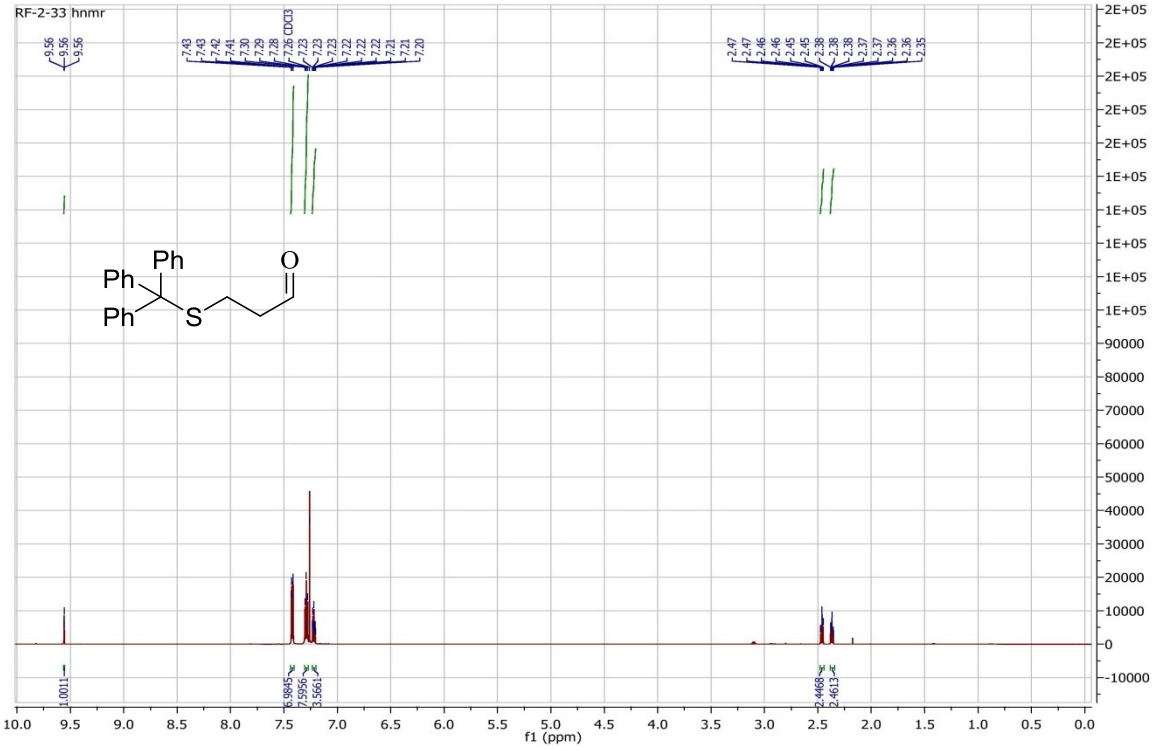

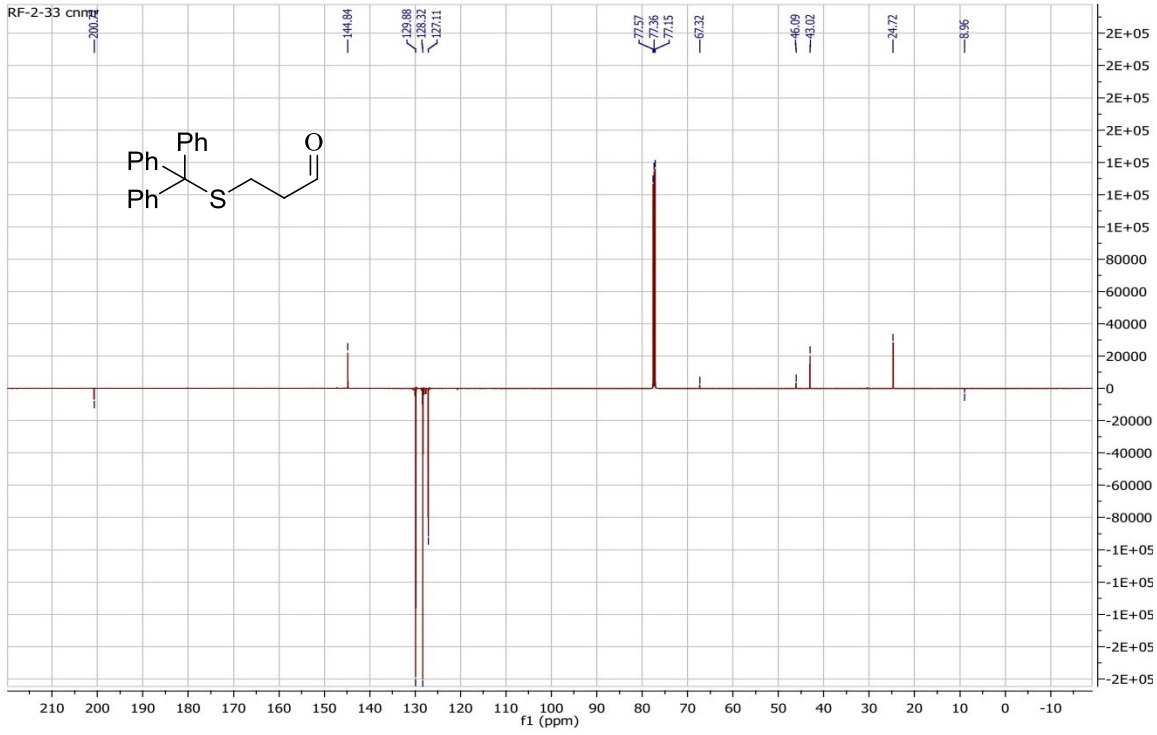

5-(tritylthio)pent-2-enenitrile (7).

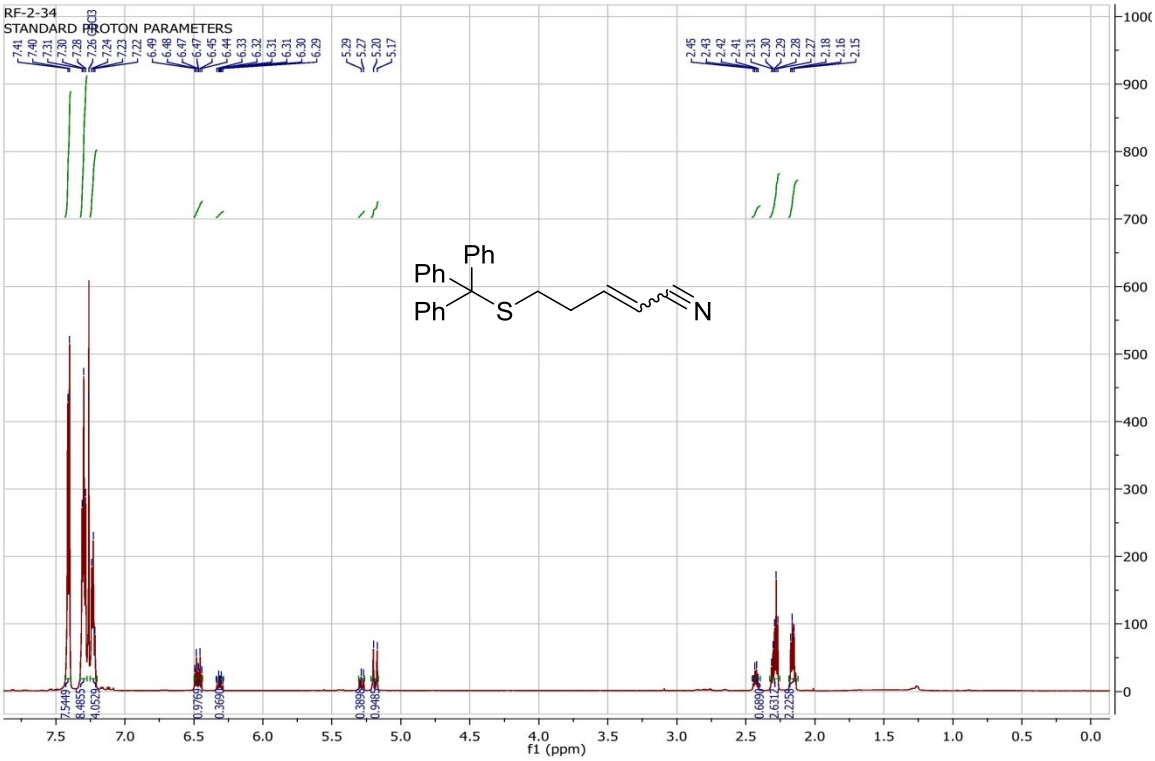

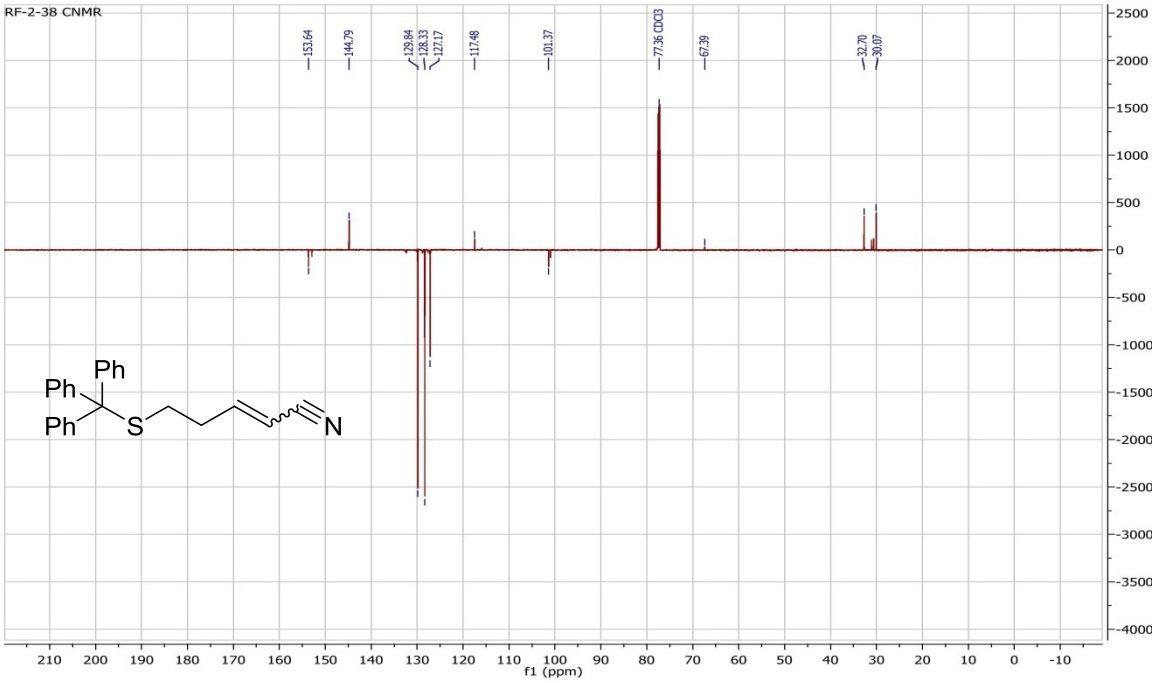

(E)-5-(tritylthio)pent-2-enal (8).

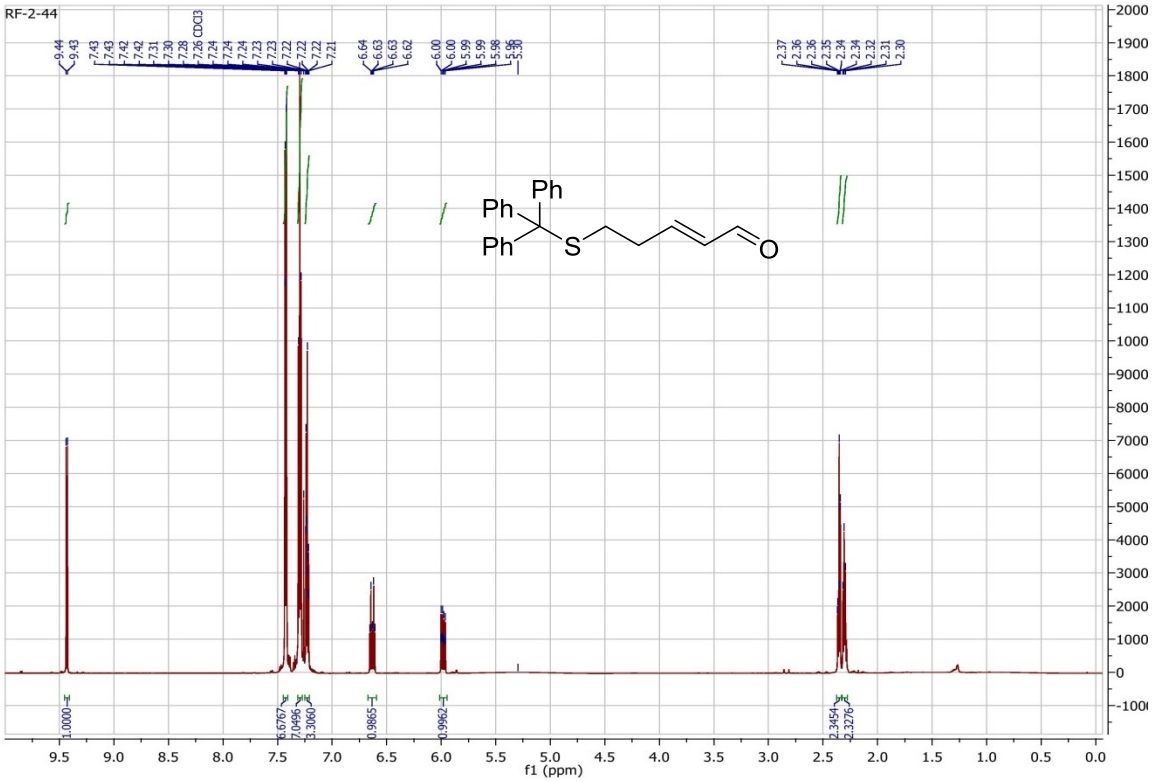

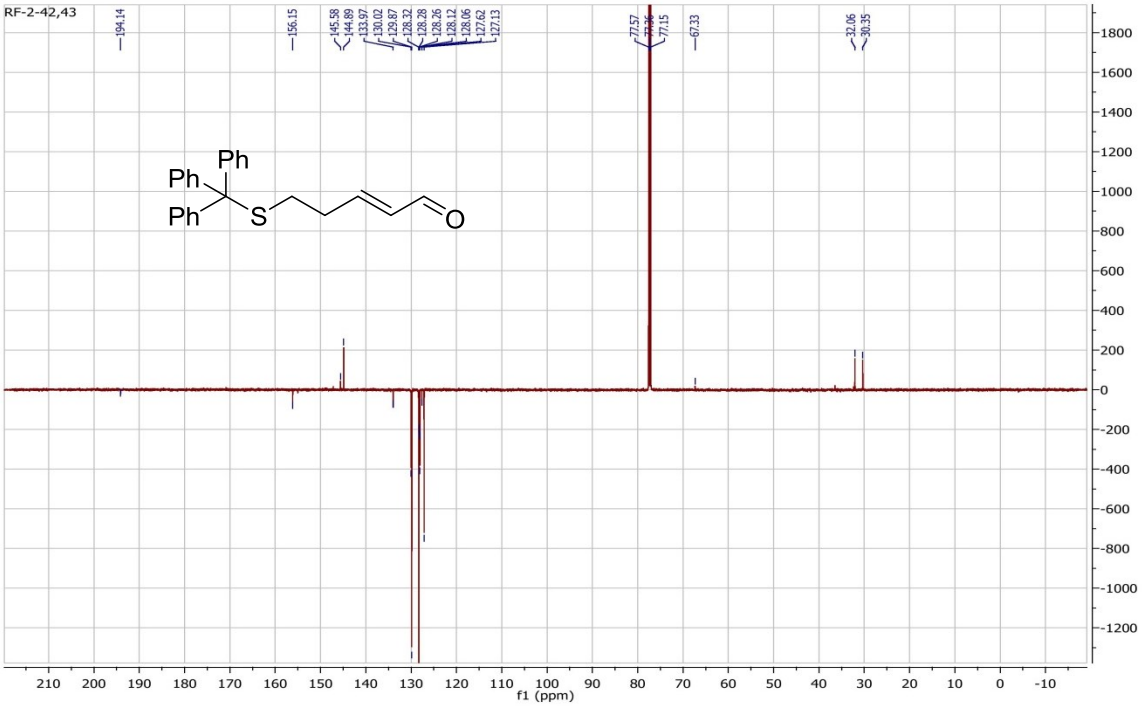

(6-(Hydroxymethyl)pyridine-2-yl)methyl 4-methylbenzenesulfonate (10).

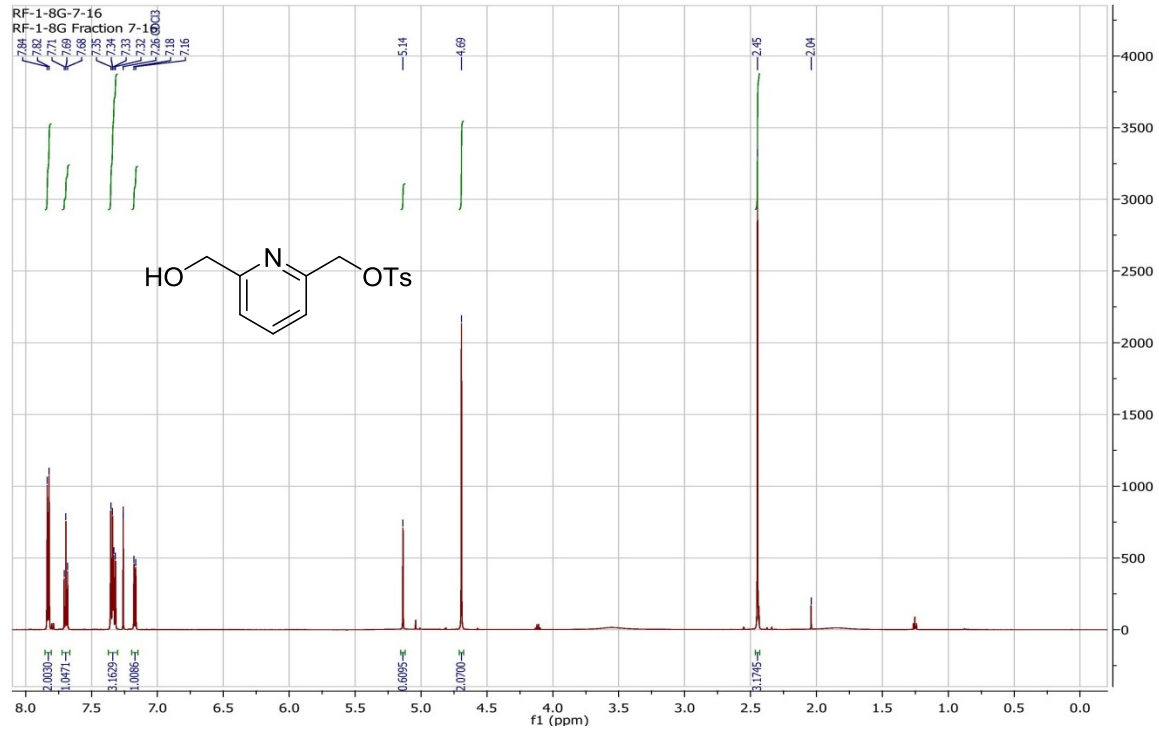

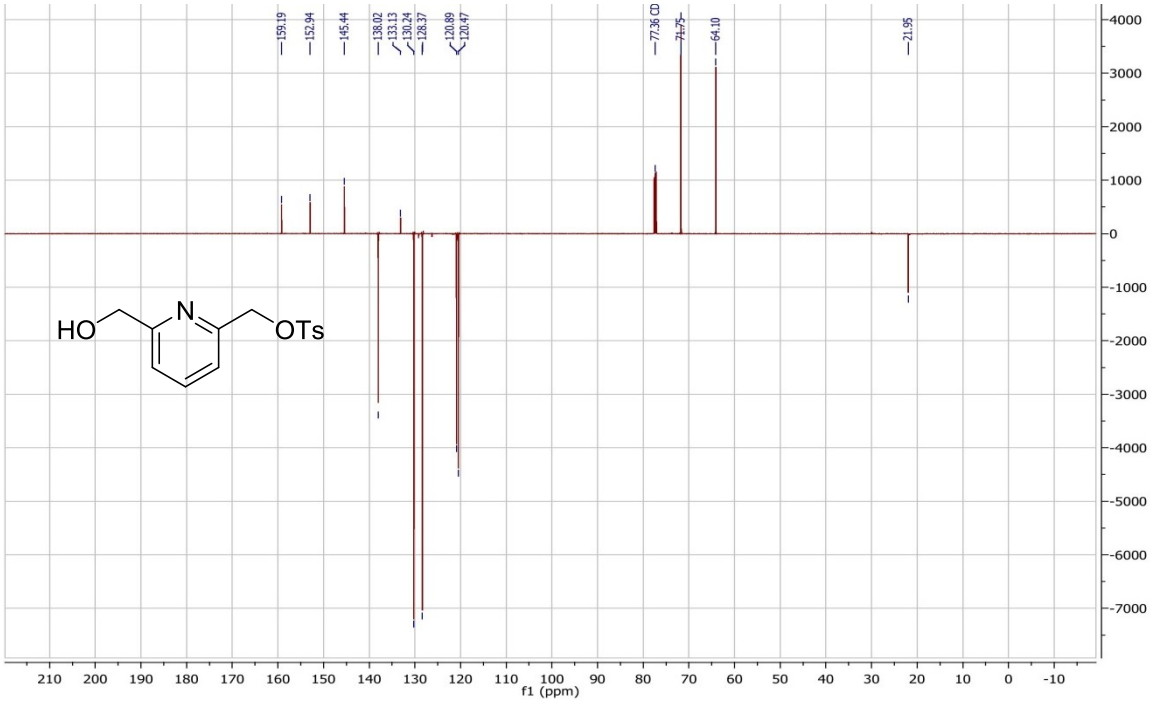

(6-(azidomethyl)pyridine-2-yl)methanol (11).

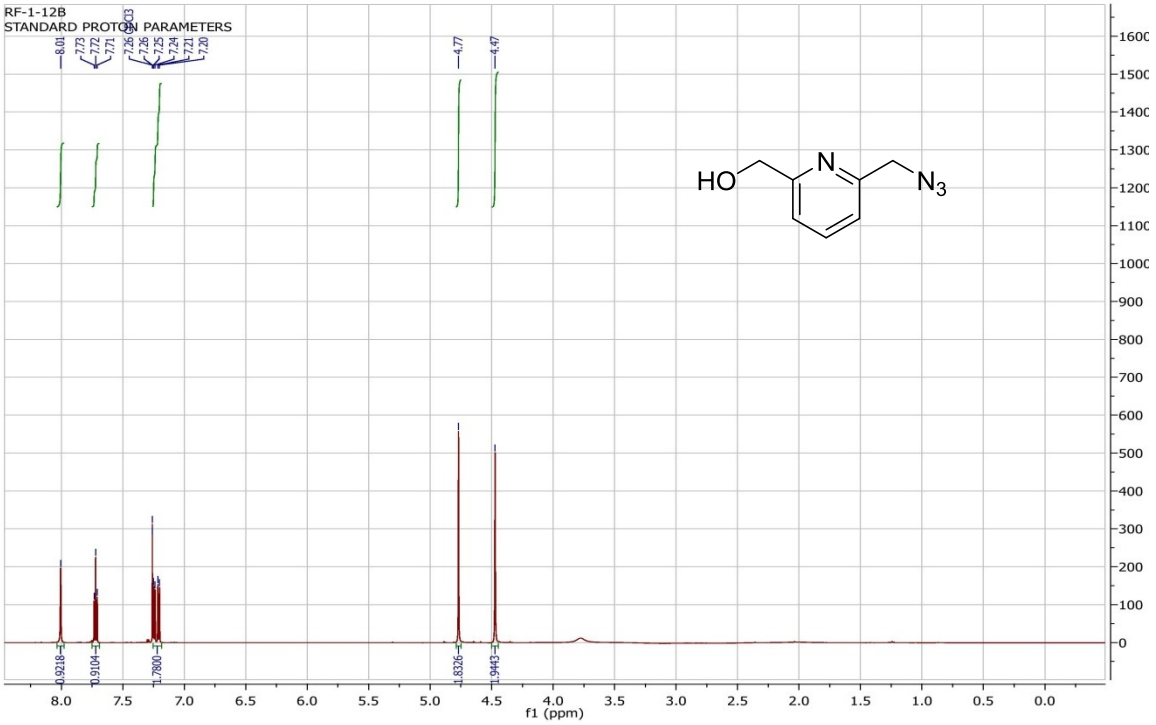

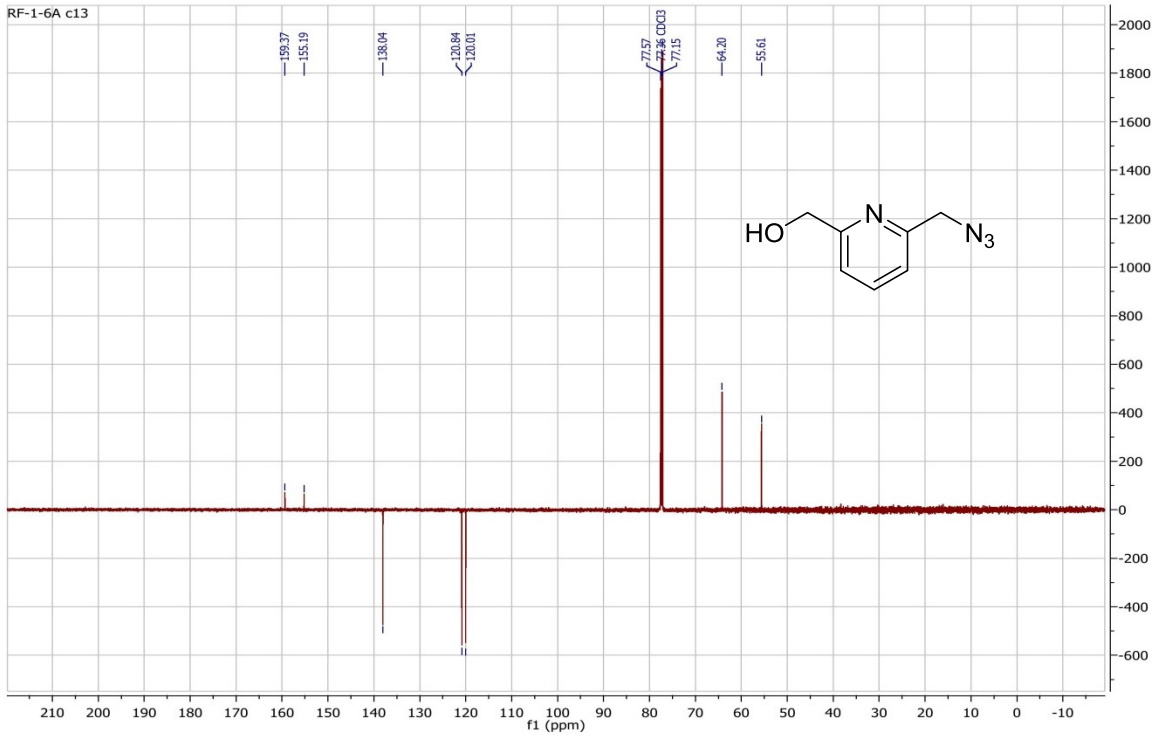

(6-(azidomethyl)pyridine-2-yl)methyl 4-mehylbenzenesulfonate (12).

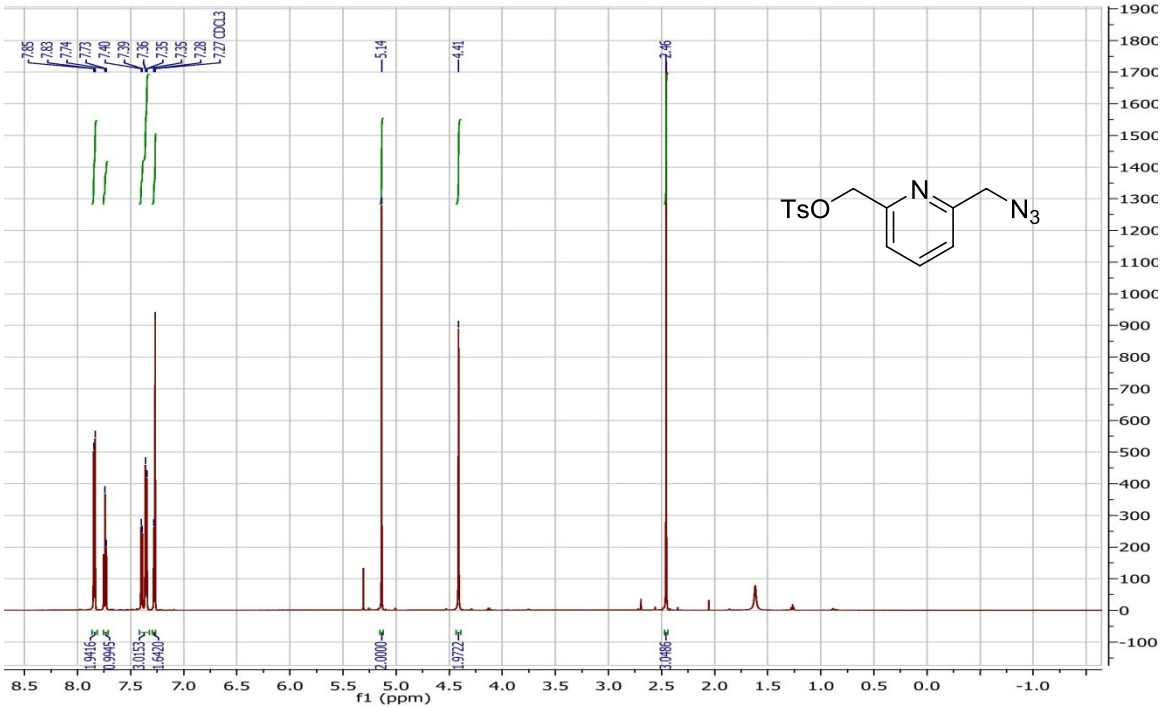

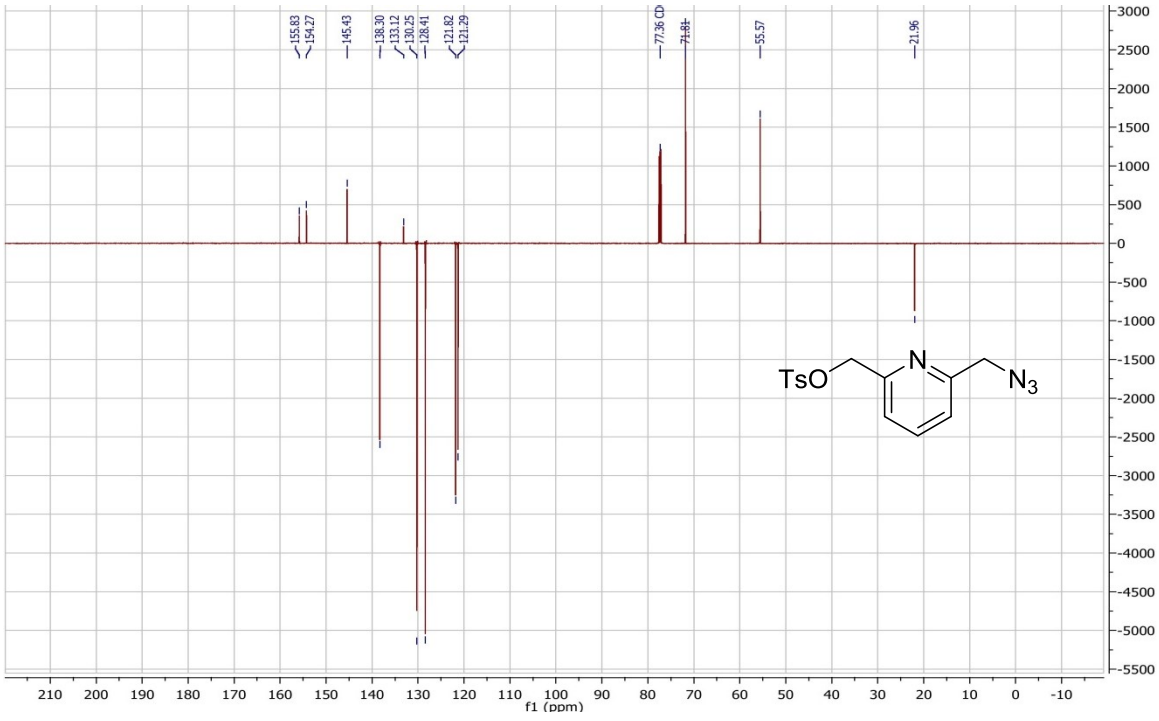

(S<E)-3-Hydroxy-1-((R)-4-isopropyl-2-thioxothiazolidin-3-yl)-7-(tritylthio)hept-4-en-1-one (13).

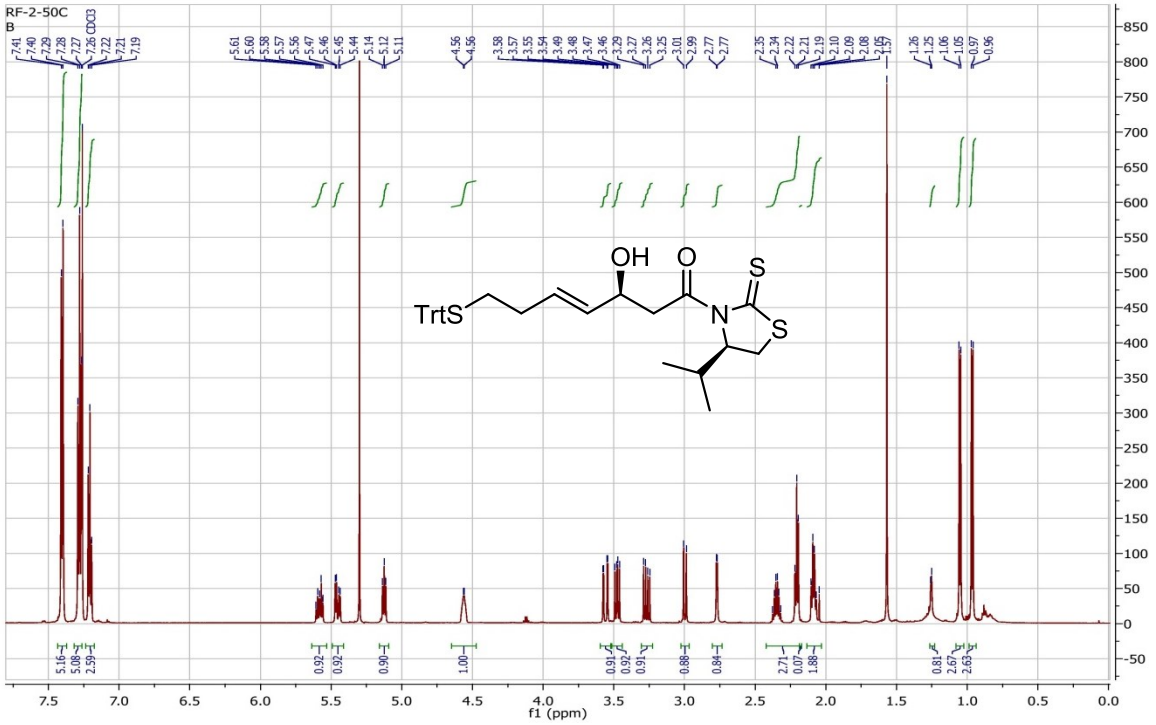

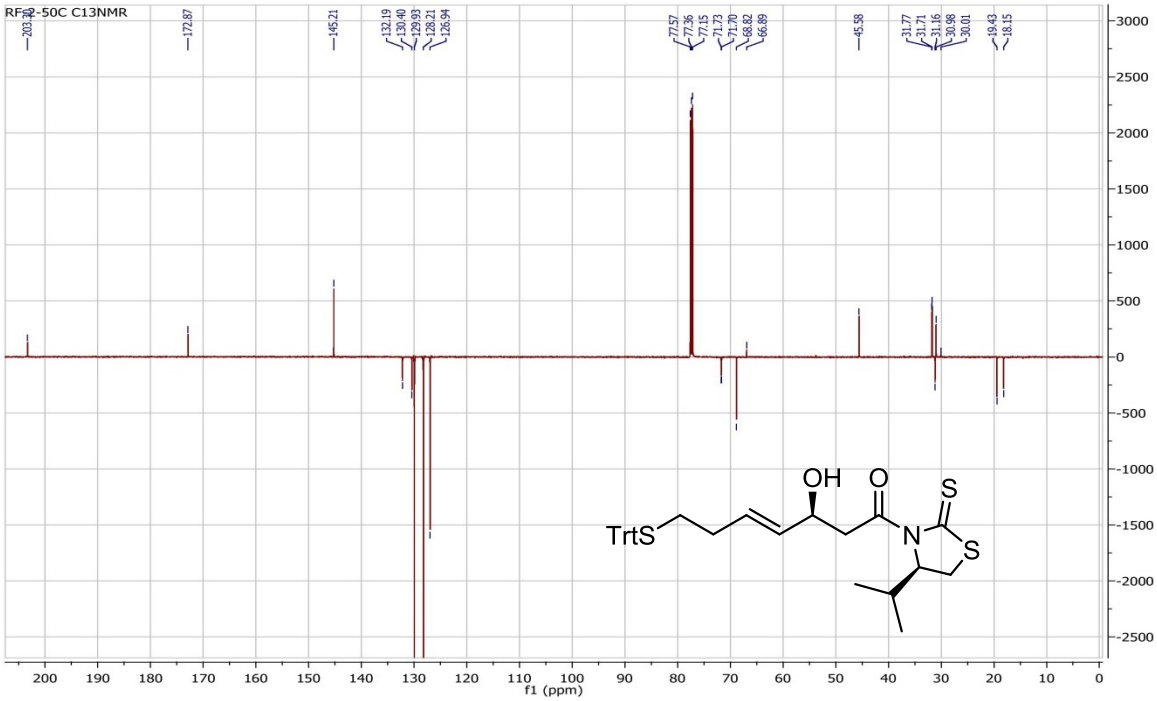

2-(Trimethylsilyl)ethyl 2-bromoacetate (16).

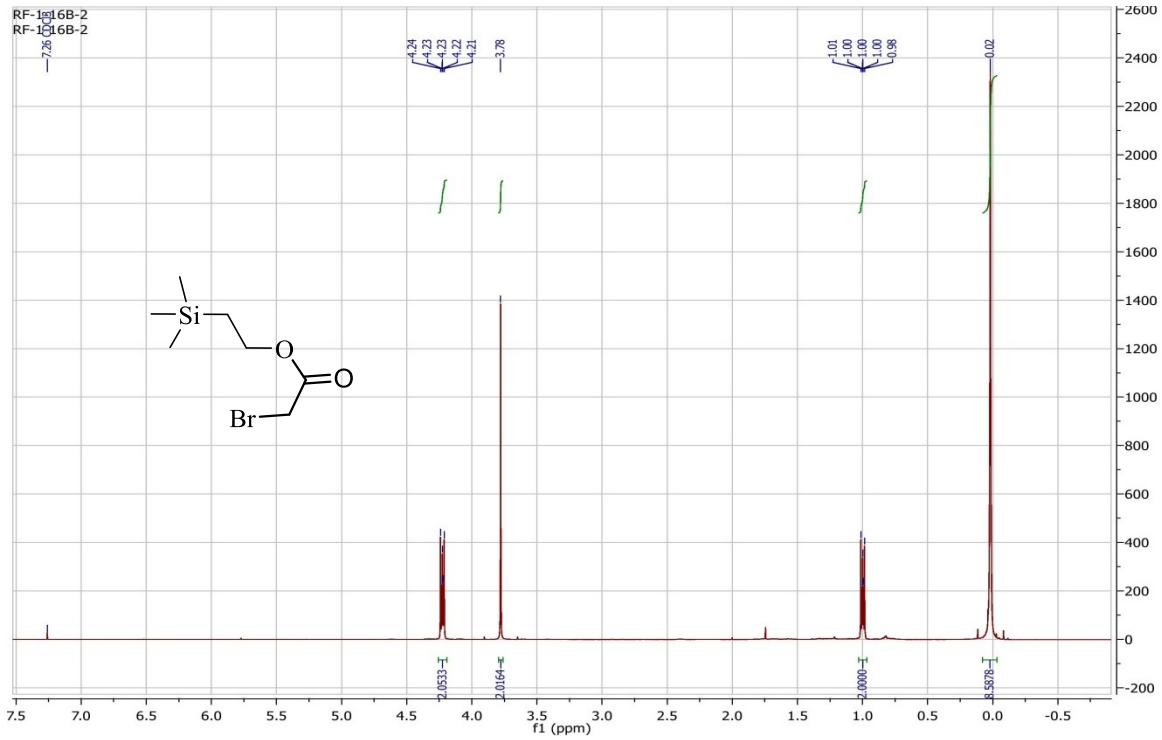

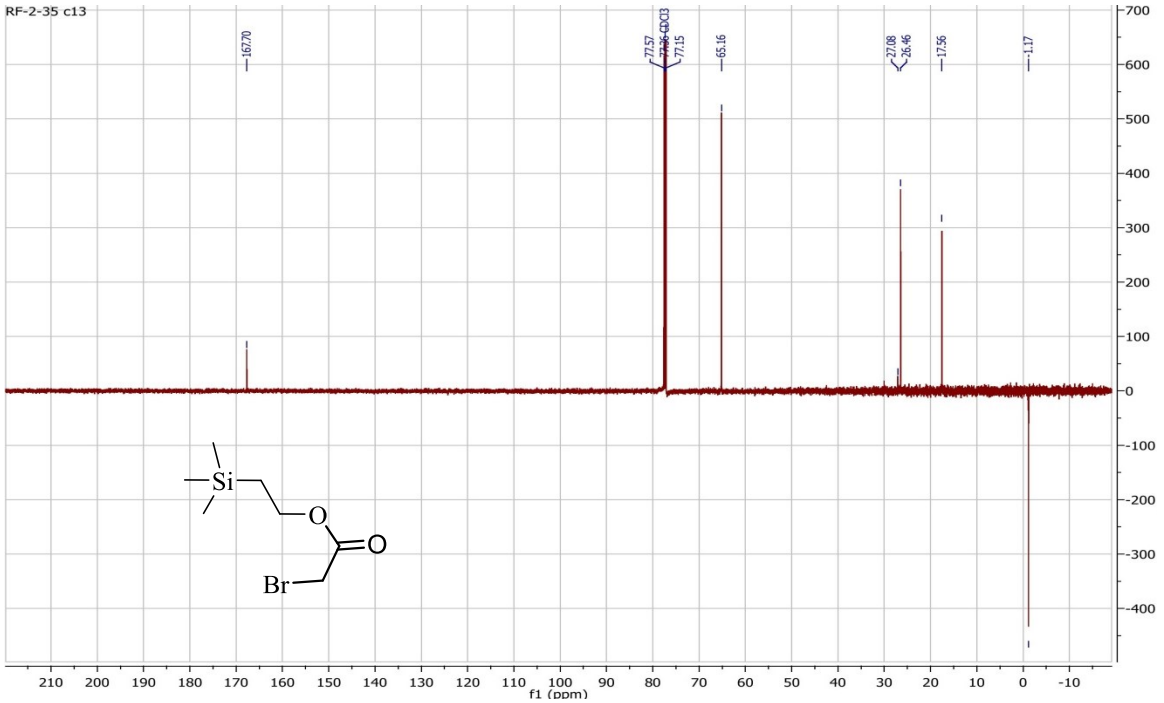

2-(Trimethylsilyl)ethyl (4-methylbenzyl)glycinate (18).

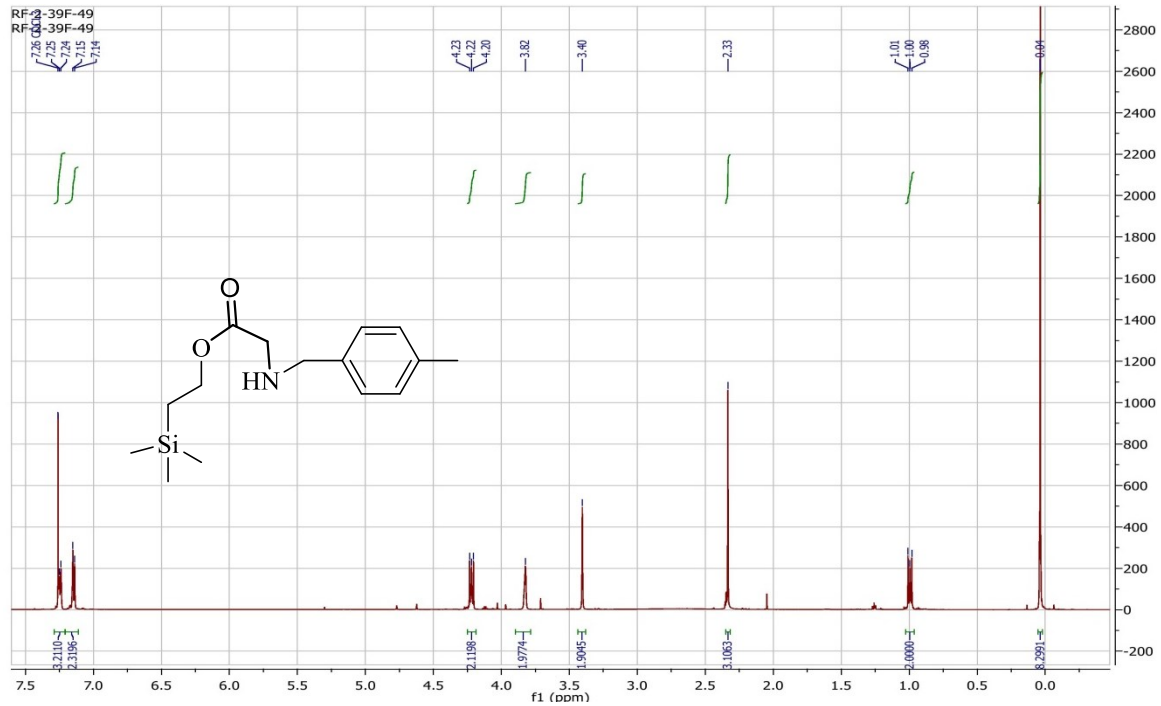

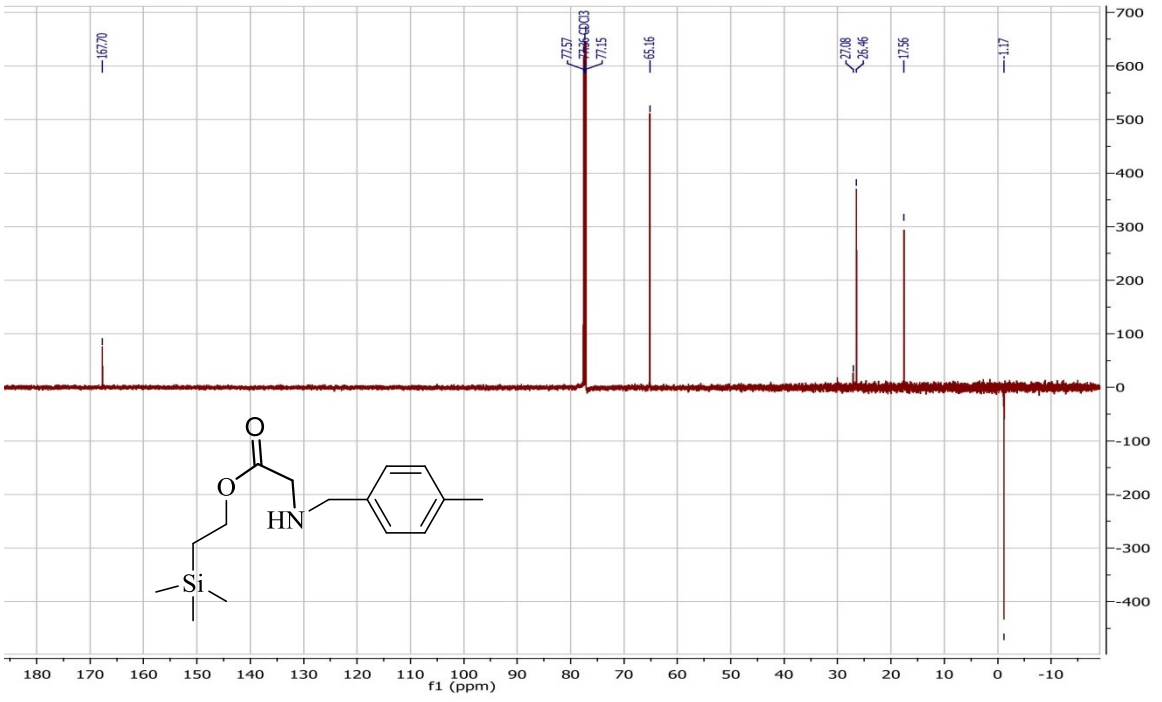

2-(Trimethylsilyl)ethyl *N*-((6-(azidomethyl)pyridine-2-yl)methyl)-*N*-(4-methylbenzyl)glycinate (19).

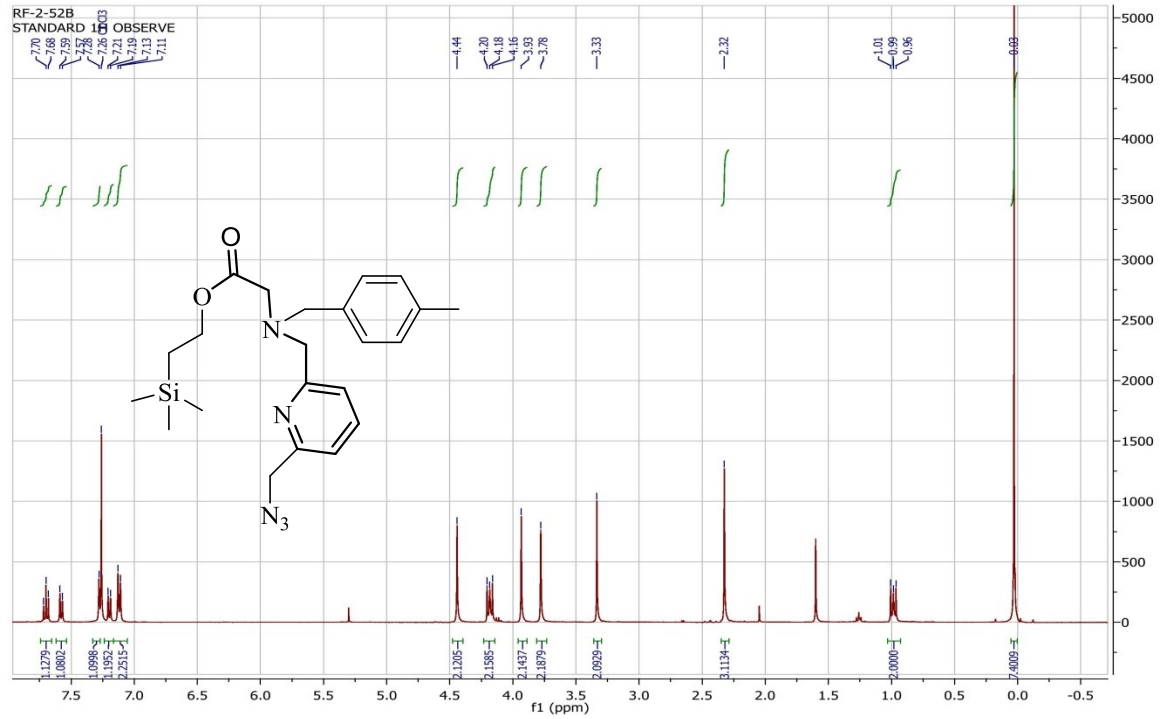

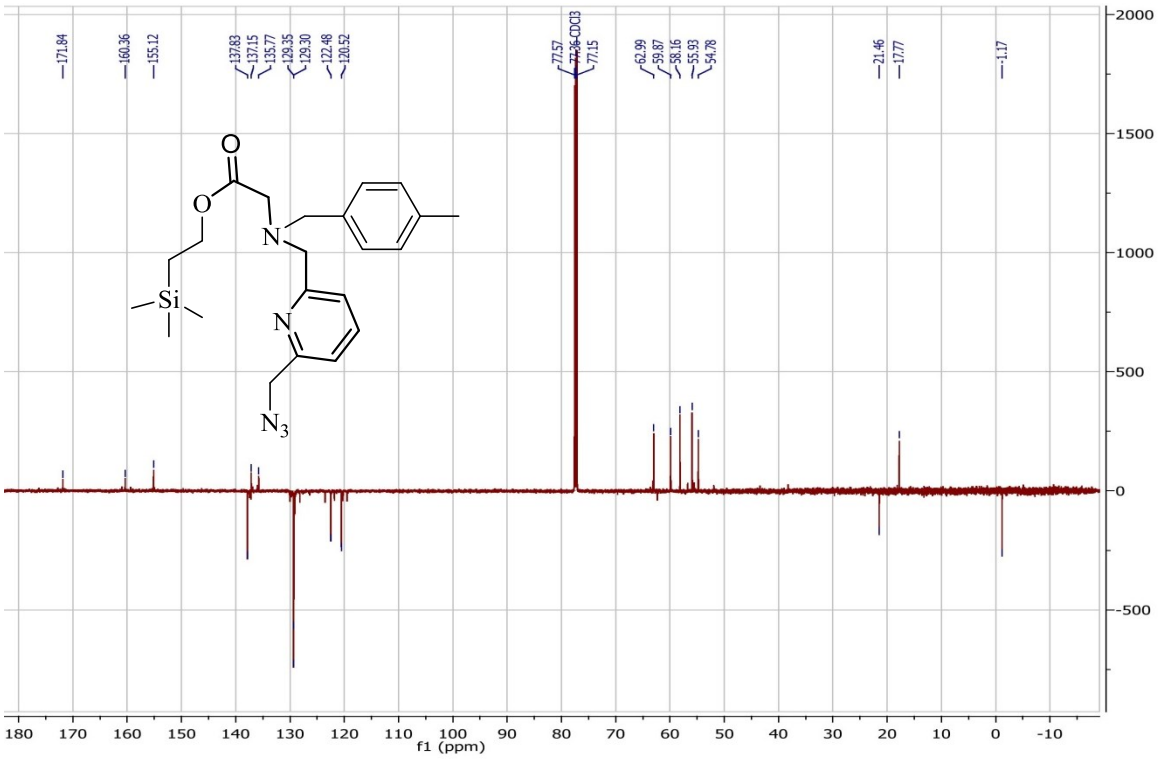

2-(Trimethylsilyl)ethyl *N*-((6-(aminomethyl)pyridine-2-yl)methyl)-*N*-(4-methylbenzyl)glycinate (20).

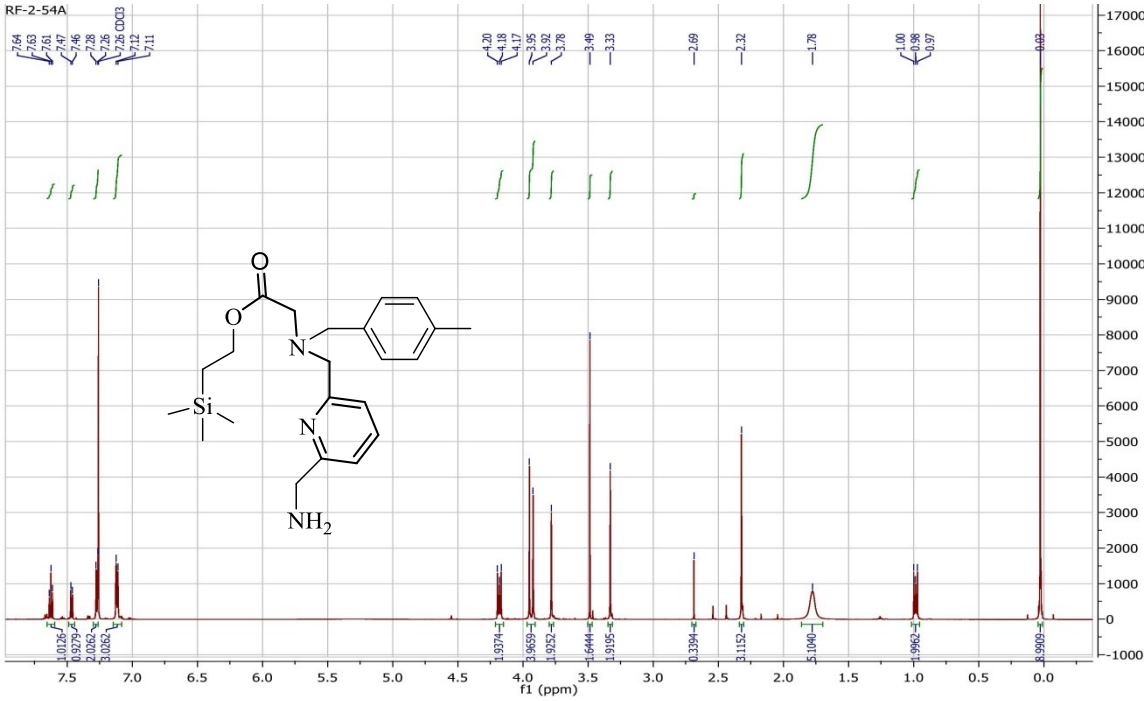

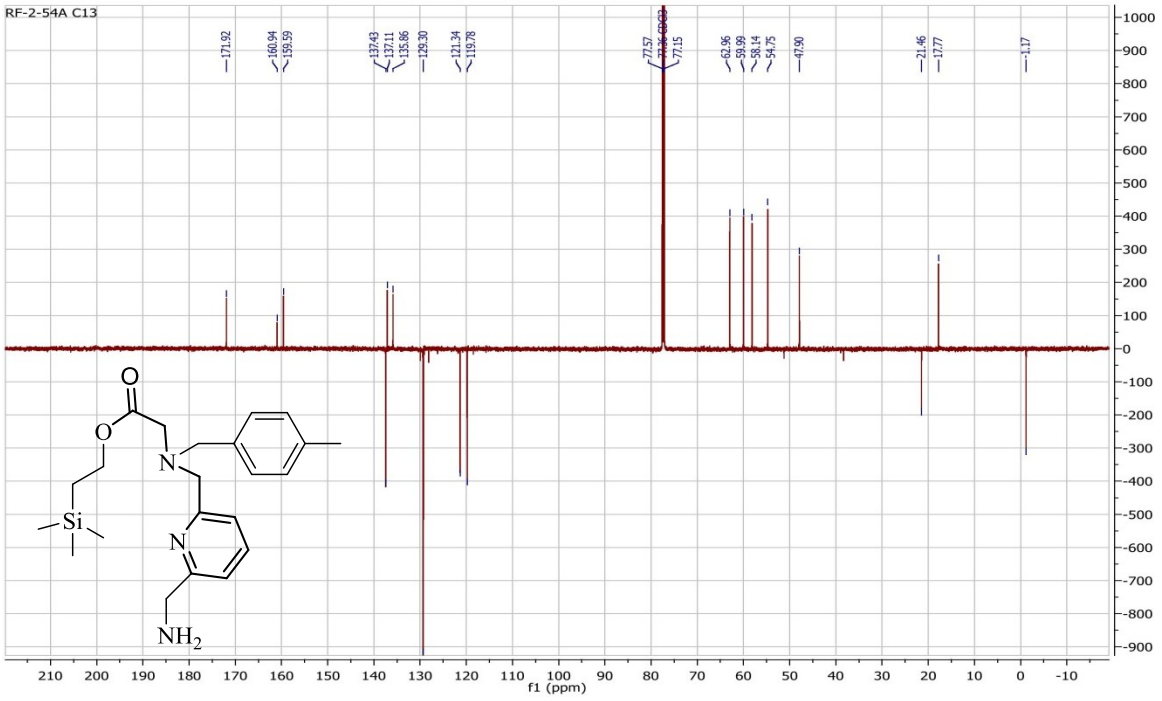

2-(Trimethylsilyl)ethyl (*S*,*E*)-*N*-((6-((3-hydroxy-7-(tritylthio)hept-4-enamido)methyl)pyridine-2-yl)methyl)-*N*(-methylbenzyl)glycinate (21).

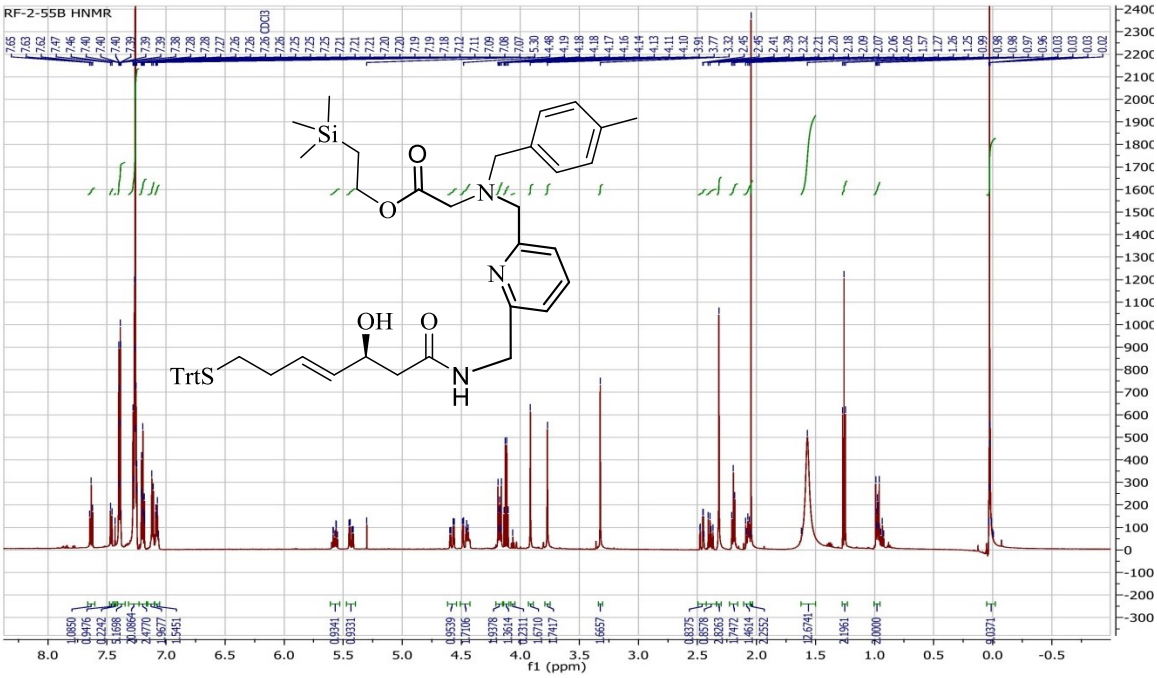

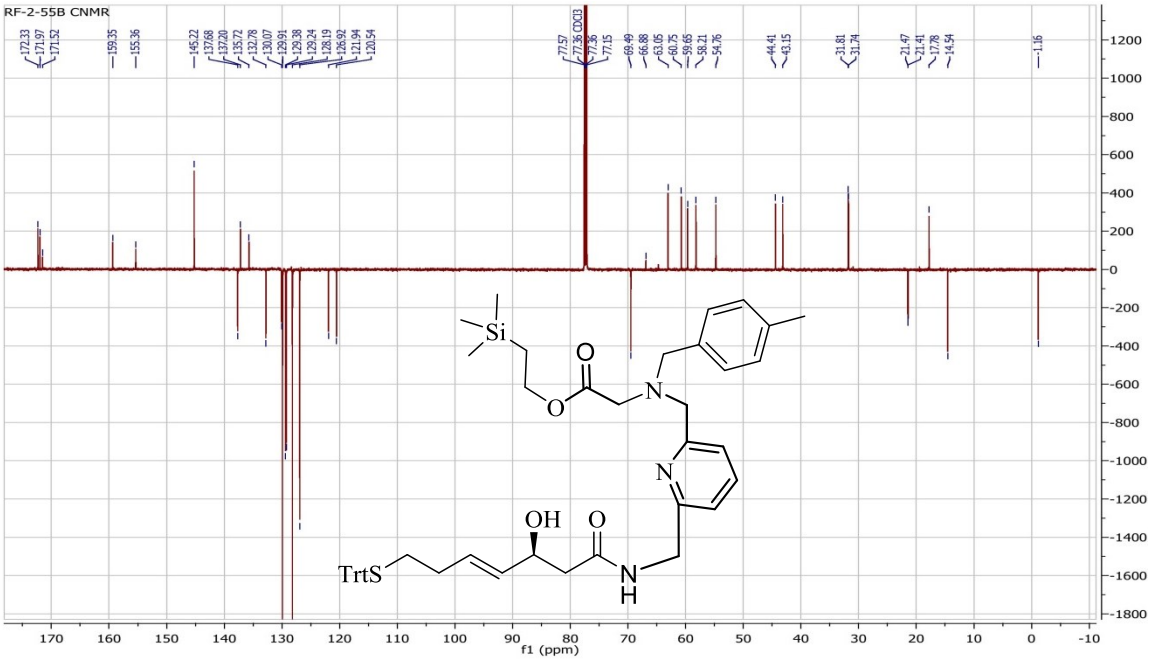

(*S*,*E*)-1-(((6-(((4-Methylbenzyl)(2-oxo-2(2-(trimethylsilyl)ethoxy)theyl)amino)methyl)pyridin-2-yl)methyl)amino)-1-oxo-7-(tritylthio)hept-4-en-3-yl (((0H-fluoren-0-yl)methoxy)carbonyl)-D-valinate (23).

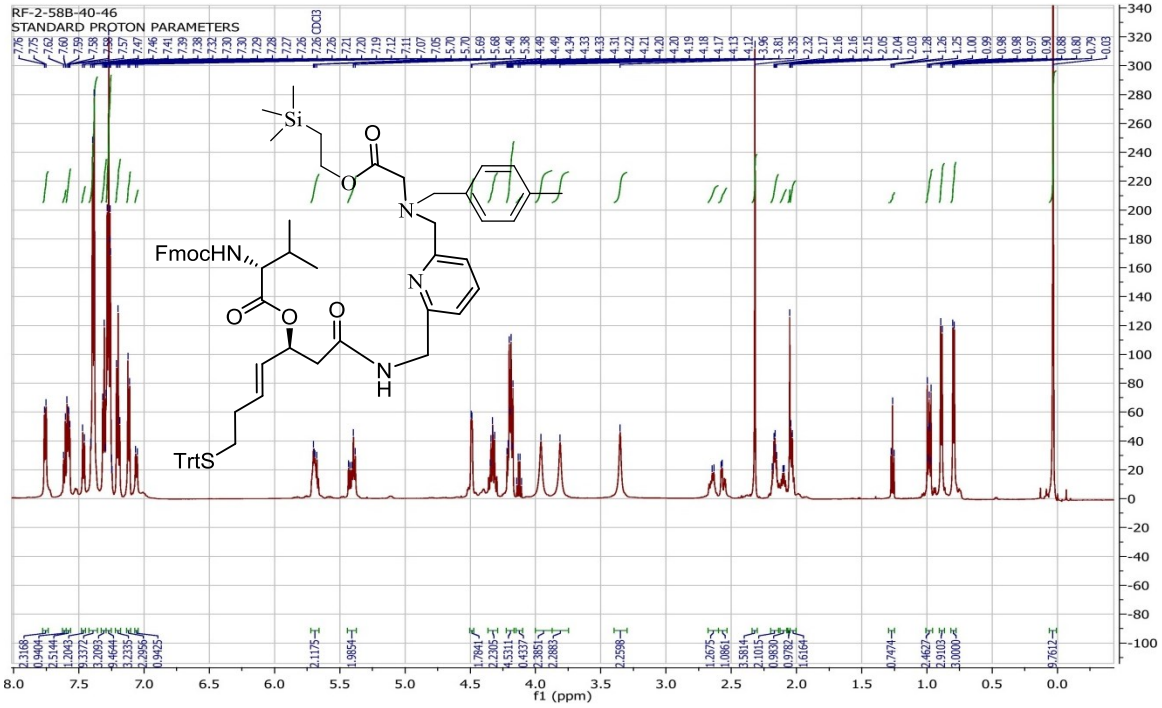

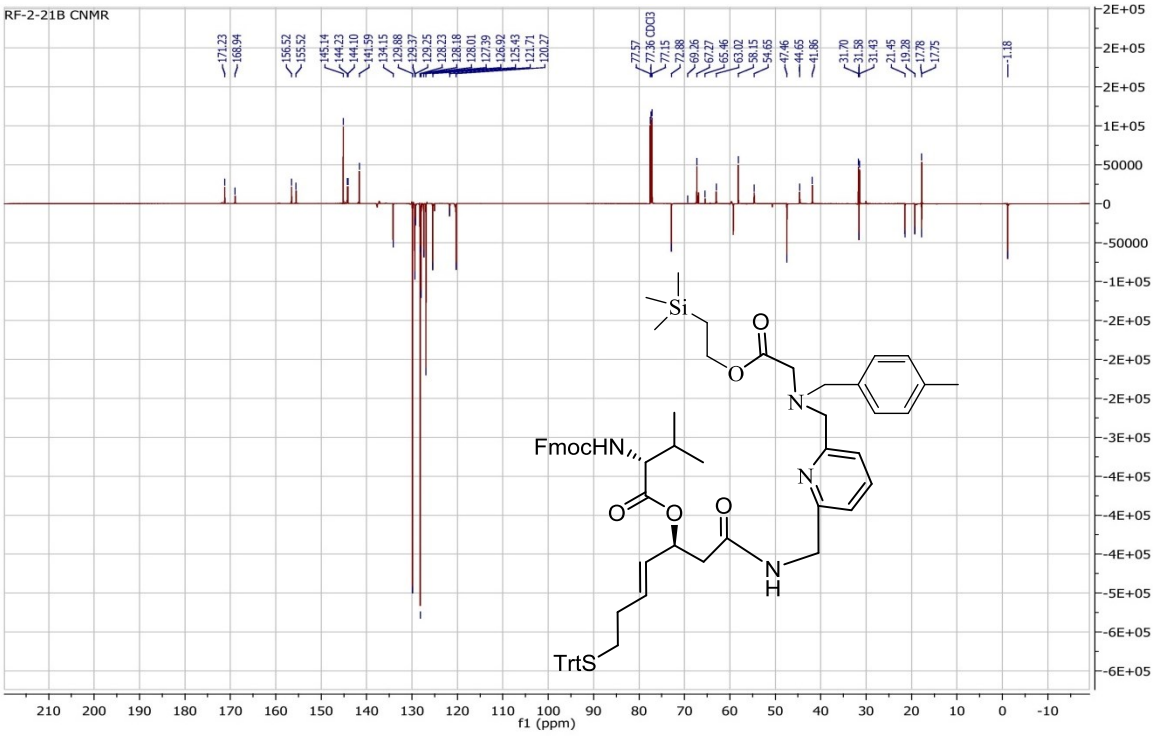

(7*S*,10*S*)-7-Isopropyl-3-(4-methylbenzyl)-10-((E)-4-(tritylthio)but-1-en-1-yl)-9-oxa-3,6,13-triaza-1(2,6)-pyridinacycloetetradecaphane05,8,12-trione (24).

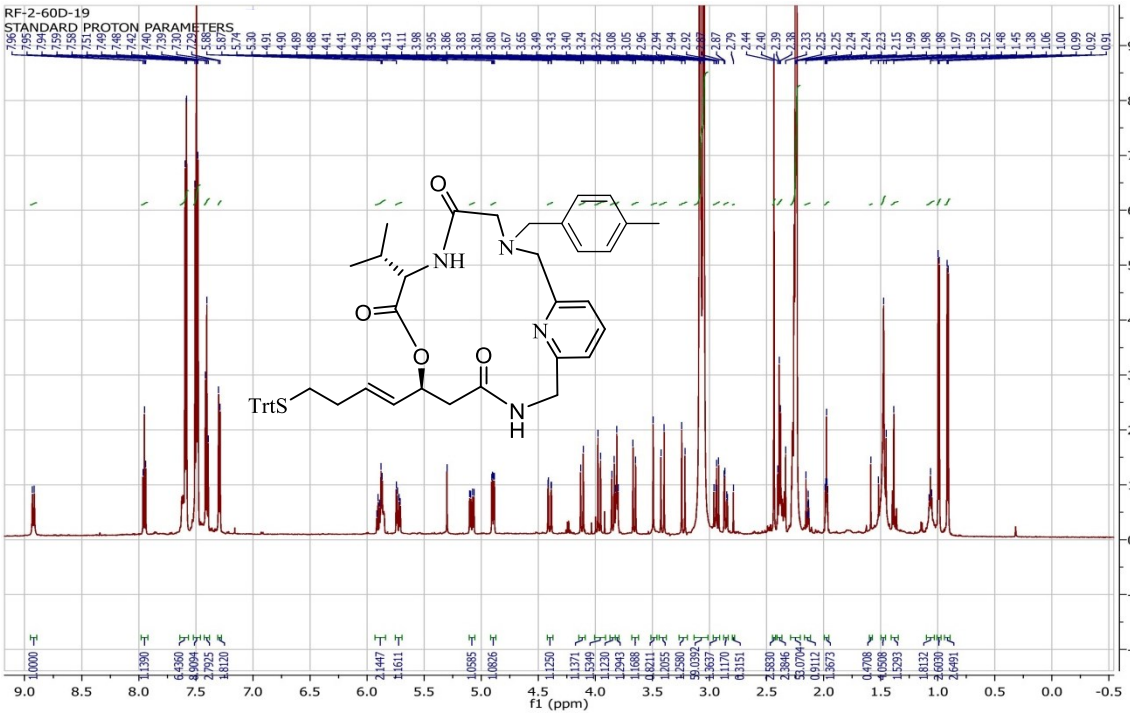

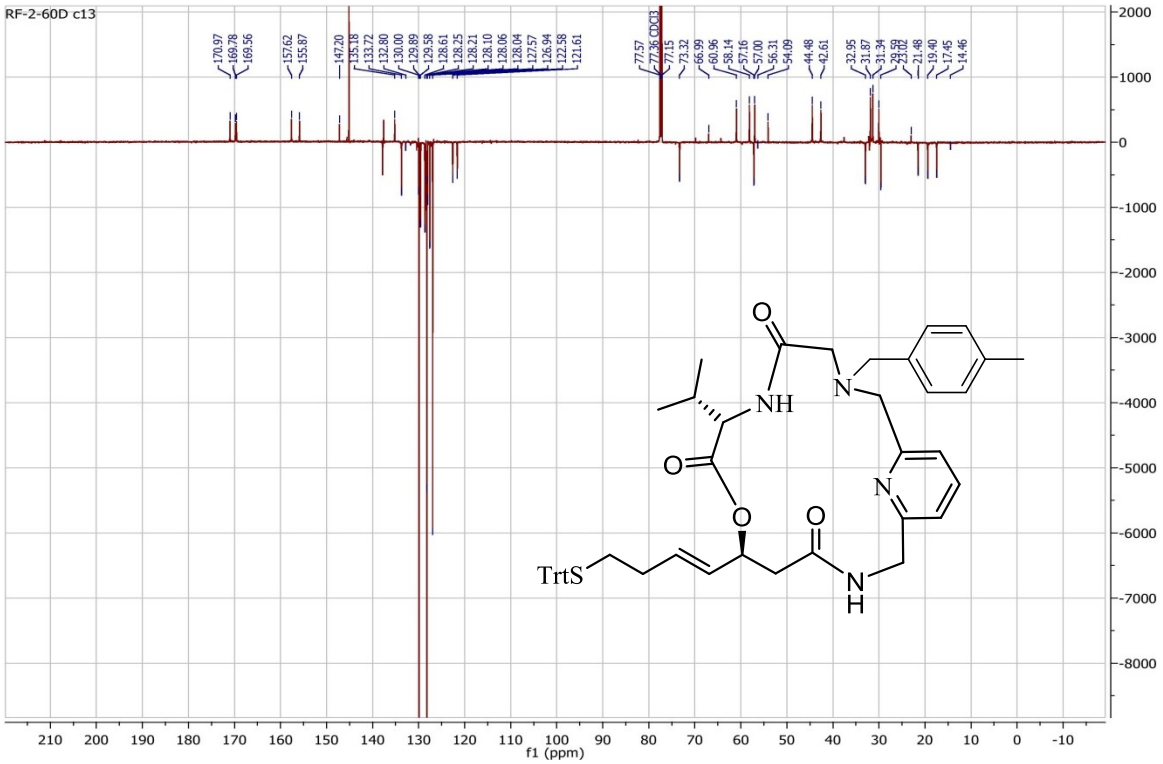

S-((E)-4-((7S,10S)-7-Isopropyl-3-(4-methylbenzyl)-5,8,12-trioxo-9-oxa-3,6,13-triaza-1(2,6)-pyridinacyclotetradecaphane-10-yl)but-3-en-1-yl) octanethioate (RF1).